The $\sigma\tau_+$ Strength in Nuclei

Dongwoo Cha

Michigan State University

1982

ABSTRACT

THE $\sigma\tau_+$ STRENGTH IN NUCLEI

By

Dongwoo Cha

The $\sigma\tau_+$ strength function is studied by the quasi-particle random phase approximation. When applied with a zero-range interaction, it is found that the particle-hole interaction reduces the unperturbed $\sigma\tau_+$ strength by a factor of about two uniformly across the whole range of the excitation energy, while the particle-particle interaction removes part of the strength from the lowest excitation to higher excitation energy region. By comparing the theory with the observed log(ft) values of the β^+ decay in medium heavy neutron rich nuclei, we found that the strong quenching, which is present in other isovector spin-flip transitions, is also required for the $\sigma\tau_+$ mode. Finally, we predict that there is a large concentration of the $\sigma\tau_+$ strength at high excitation energy which can not be accessed by the β^+ decay.

THE $\sigma\tau_+$ STRENGTH IN NUCLEI

By

Dongwoo Cha

A THESIS

Submitted to
Michigan State University
in partial fulfillment of the requirements
for the degree of

DOCTOR OF PHILOSOPHY

Department of Physics

1982

To my mother

ACKNOWLEDGEMENTS

I am greatly indebted to Professor George Bertsch, my thesis advisor, who has suggested this problem to me, and guided, inspired, and supported me through the whole period of my graduate study at Michigan State University.

I would like to thank Professor Hobson Wildenthal and Dr. Hans Kruse for their assistance in using the shell model code, Professors N. Anantaraman and Ikuko Hamamoto for helpful discussions, and Professor Jerzy Borysowicz for his concern and valuable advice during the early stages of my graduate work.

Special thanks are also due to Professor Hiroshi Toki for helping me whenever I ran into a problem, encouraging me when I was discouraged, and paying close attention to my progress.

Mrs. Holly Husted has read the entire manuscript and corrected English to this readable form.

Finally, I would like to thank my wife Shinwon for her patience and understanding during this period in our lives when our time together has been in short supply, and my daughter Seungyun and my son Sahnghyun for greeting me faithfully each morning and evening.

TABLE OF CONTENTS

LIST OF TABLES

LIST OF FIGURES

Chapter I

INTRODUCTION

One of the most important achievements in nuclear physics in recent years is the progress made in the understanding of spin excitations in nuclei. On the experimental side, intermediate energy (100∿200 MeV) hadronic probes make it possible to observe spin-flip isovector excitations in nuclei selectively. From measurements at very forward angles, the prominent spin-flip states with L=0 can be distinguished very effectively. Furthermore, the spin independent part of the effective isovector interaction decreases significantly for the above bombarding energies while that of the spin dependent part stays close to constant, and therefore the spin-flip states become more conspicuous. [Lov81]

On the theoretical side, a large concentration of the spin-flip strength has been predicted since as early as the 1960's to account for the strong hindrance of the allowed Gamow-Teller (GT) β decay. [Ike63] This is a straight analogy of the isobaric analog state (IAS) which depletes much of the strength of the allowed Fermi decay, or the electric giant dipole resonance, related to first forbidden β decay. [Gaa80]

After searching more than a decade, the giant GT

resonance in medium heavy nuclei was finally found in 1975 by Doering et al. using the (p,n) reaction at 45 MeV. [Doe75] The spin-flip without charge-exchange was first observed in heavy nuclei in 1981 when Anantaraman et al. measured the M1 resonances in Zirconium isotopes by the inelastic scattering of 200 MeV protons. [Ana81] Now, enough data have been accumulated to draw a definite description of the nature of the spin and isospin dependent part of the nuclear interaction. [Bai80, And80, Hor80, Ste80, Ori81, Goo81, Cra82, Ana82] They give information not only on the nuclear structure itself but also on the mesonic phenomena such as that leading to pion condensation. This is because the quantum numbers involved are the same as those of the nuclear spin-flip and isospin-flip states. [Mey81] In fact, studies so far show concrete evidence that the isovector spin-flip strength, both the GT and M1 strength, in medium heavy nuclei is strongly quenched by a factor of about three with respect to the shell model estimation. [Knu80, Blo81, Goo81, McG81, Kre81, Cra82, Sag82, Ana82] The mechanism for this extra strength reduction must be found somewhere outside the present model space, for example from the collective Δ-hole excitations, [Boh81, Bro81] or from more complex configurations. [Ber82a] But it has been stressed [Wei82] that we should first know that the nuclear structure calculation is correct before making quantitative estimation of the more exotic mechanisms for strength reduction.

The spin-flip isovector operator has three modes, namely, two charge-exchange modes $\sigma\tau_{\pm}$ (the GT transition) and one non-charge-exchange mode $\sigma\tau_{o}$ (the M1 transition). Though the same reaction mechanism governs them all, the transition strength realized in three adjacent isobaric nuclei may look very different due to the ground state configuration of the parent nucleus. The difference between the $\sigma\tau_{+}$ and the $\sigma\tau_{-}$ strength tells us about the asymmetry between neutrons and protons present in the initial ground state. In medium heavy nuclei, usually a large neutron excess is built up. So the $\sigma\tau_{-}$ strength would be large with most of them originated from this obvious neutron excess. On the other hand, the $\sigma\tau_{+}$ strength comes mainly from the ground state correlation, except for the contribution from those transitions where the $j_{>}=\ell+\frac{1}{2}$ level is occupied while the $j_{<}=\ell-\frac{1}{2}$ neutron level is empty. Therefore, there is a particular interest in studying the $\sigma\tau_{+}$ strength. Unfortunately, however, the data available at present for this mode are only from β^{+} decay. The β^{+} decay can only provide limited information on the strength function at the tail region of the spectrum whose energy is less than the Q-value.

The β decay in medium heavy nuclei has been studied by many authors. Kisslinger and Sorensen applied the pairing theory to the β decay of spherical heavy nuclei for the first time. [Kis63] They showed that the isotope dependence

of the log(ft) values can be explained simply by the occupation probabilities in the Bardeen-Cooper-Schrieffer (BCS) ground state. Hamamoto investigated the β decay in odd mass nuclei by the perturbation theory admixing a one-quasiparticle (QP) state with three-QP states. [Ham65] It was shown that her results depend sharply on the strength of the residual interaction. Halbleib and Sorensen studied the GT β decay in odd-odd mass nuclei. [Hal67] They adopted the pairing plus quadrupole force between like nucleons and the short-range δ-force and/or the long-range GT force between unlike nucleons and could reproduce the data within a factor of three. Klapdor and Wene were the first to point out that the structure of the low-lying part of the strength function can have a strong effect on the predictions such as β decay half lives and astrophysical calculations. [Kla80] Klapdor et al. calculated the strength function for many heavy nuclei around the line of β stability using a schematical interaction. [Kla81] By using their model, they found that the half lives for neutron rich nuclei are systematically shorter than obtained by simpler models.

In this thesis, we want to study the $\sigma\tau_+$ strength function for even-even nuclei with a large neutron excess between mass numbers A=100∿150. We shall compare it with the data from the β^+ decay. Our model theory is the QP random phase approximation (RPA) for particle-hole (PH) states of unlike nucleons. As for single particle wavefunctions, we

shall use the BCS wavefunctions from a Woods-Saxon (WS) potential assuming the pairing correlation between like nucleons only. The pairing correlation in the ground state of the parent nucleus plays a very important role, in addition to the ground state correlation for the β^+ decay of neutron rich nuclei. Without it, either there would be no available empty neutron levels for the transition or the transition energy would be in most cases too large to appear as a decay. As for the residual interaction, we will take only the central part of the interaction in the zero-range approximation. Besides the advantage of its simplicity in calculation, it has been shown to give good agreement with the GT and the M1 states. [Ber81a, Tok81]

We start this thesis keeping the following goals in mind:

i) to reproduce the observed log(ft) values of the β^+ decay in medium heavy neutron rich nuclei;

ii) to confirm the extra reduction in strength which has no explanation within the shell model description;

iii) to generate the $\sigma\tau_+$ strength function above the Q-window which may be tested by future experiments such as the (n,p) reaction.

We will first review the characteristics of the GT transition and present the results of recent (p,n) and (p,p') experiments in Chapter II. The QP-RPA for the charge-exchange mode shall be developed in Chapter III. In Chapter

IV, we shall present the details of our calculation. The results of the application of the QP-RPA on the β^+ decay of medium heavy nuclei will be the subject of Chapter V. In Chapter VI, the validity of the QP-RPA shall be tested against the full-scale shell model (FSM) calculation for the case of ^{12}C as a simulation of heavy neutron rich nuclei, followed by the conclusion in Chapter VII.

Chapter II

CHARACTERISTICS OF GAMOW-TELLER TRANSITION

2-1 Gamow-Teller transition

A charge-exchange transition can be characterized by the operator which is a particular term in the multipole expansion, namely [Eji78]

$$[Y_L(\hat{r})\times\sigma^S]^J\tau_\pm. \tag{2-1}$$

Here σ and τ are the usual spin and isospin matrices. τ_+ transforms a proton into a neutron and τ_- does vice versa. L, S, and J denote the orbital, the spin, and the total angular momentum respectively, which the outgoing particle carries off. The most dominant multipole, L=0, of (2-1) is divided into two groups: the Fermi transition where S=J=0 and the GT transition (or the $\sigma\tau_\pm$ transition) where S=J=1. In this study, we are interested in the GT transition which has the following selection rules: [Sha74, p784]

$$J'_f-J'_i=\pm1,0 \quad (0\to0 \text{ forbidden}) \tag{2-2a}$$

$$\pi_f-\pi_i=0 \tag{2-2b}$$

$$(T'_z)_f-(T'_z)_i=\pm1 \tag{2-2c}$$

where f and i denote the final and the initial state respectively, and J', π, and T' denote the total angular momentum, the parity, and the isospin of a given state respectively. T'_z has the same value for all states in a given nucleus and can be written by

$$T'_z=(N-Z)/2. \qquad (2-3)$$

The $\sigma\tau_+$ and $\sigma\tau_-$ transitions form the isovector spin-flip transition with the $T_z=0$ mode, the M1 transition. If the isospin is a good quantum number, as in doubly closed shell nuclei, then the isovector spin-flip transition has the isospin selection rule in addition to Equations (2-2) given by

$$T'_f-T'_i=\pm1,0 \quad (0\rightarrow0 \text{ forbidden}). \qquad (2-4)$$

Let us consider the jj coupling shell model. In Figure 1, we sketch the possible PH excitations for the $\sigma\tau_-$ and the $\sigma\tau_+$ transitions. They are restricted to levels with the same orbital angular momentum ℓ because of the selection rules given by Equations (2-2). We can see that Pauli blocking permits much fewer PH configurations for the $\sigma\tau_+$ transition than for the $\sigma\tau_-$ transition. The former is possible only when the $j_>=\ell+\frac{1}{2}$ level is occupied while the $j_<=\ell-\frac{1}{2}$ level is empty. The GT transition strength B(GT) between levels j_1 and j_2 is given by [Boh69, p83]

Figure 1 Possible particle-hole excitations for (a) the $\sigma\tau_-$ and (b) the $\sigma\tau_+$ transitions.

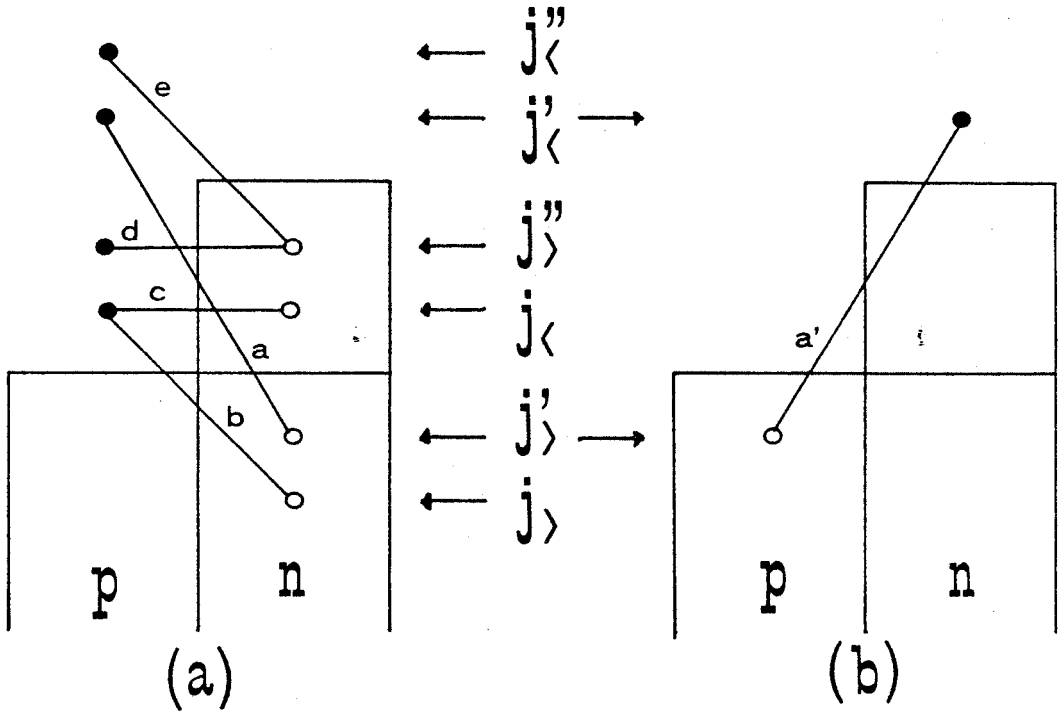

$$B(GT;j_1\rightarrow j_2)=\sum_{\mu M}|<(j_1^{-1}j_2)1M|\sigma_\mu\tau_\pm|0>|^2$$
$$=2|<j_1||\sigma||j_2>|^2. \qquad (2\text{-}5)$$

The transition rate for the β decay process is customarily expressed in terms of the product ft where t is the half life and f is a dimensionless quantity which depends on the nucleus and the transition. Since only the GT transition contributes to the allowed β^+ decay for heavy nuclei with a large neutron excess, there is a simple realationship between B(GT) and ft given by [Boh69, p410]

$$ft=\frac{2D}{(g_A/g_V)^2B(GT)} \qquad (2\text{-}6)$$

where D is a universal constant given by

$$D=\frac{2\pi^3\hbar^7\ln 2}{g_V^2m_e^5c^4} \qquad (2\text{-}7)$$

and g_A and g_V denote the coupling constants for the axial vector and the vector currents respectively. The square of the reduced matrix elements is expressed in terms of ℓ by [Law80, p433]

$$|<j_1||\sigma||j_2>|^2\begin{cases}=2(\ell+1)(2\ell+3)/(2\ell+1) & \text{when } j_1=j_2=j_>\\ =2\ell(2\ell-1)/(2\ell+1) & \text{when } j_1=j_2=j_<\\ =8\ell(\ell+1)/(2\ell+1) & \text{when } j_1=j_>,\ j_2=j_<\\ & \quad \text{or } j_1=j_<,\ j_2=j_>\end{cases} \qquad (2\text{-}8)$$

where the exact overlap of the spacial wavefunctions between the levels j_1 and j_2 is assumed. From this equation we can

find the relative importance of PH excitations. The most dominant configuration in the $\sigma\tau_-$ strength is the transition from an occupied neutron level where j has the highest value. It also follows from Equation (2-8) that the sum of the strength of transitions b and c or d and e in Figure 1 is proportional to the number of neutrons in the valence orbits, i.e.,

$$B(GT;j_>\rightarrow j_<)+B(GT;j_<\rightarrow j_<)=12\ell=6(2j_<+1) \tag{2-9a}$$

$$B(GT;j_>''\rightarrow j_>'')+B(GT;j_>''\rightarrow j_<'')=12(\ell''+1)=6(2j_>''+1)\,. \tag{2-9b}$$

Since both of the $\sigma\tau_-$ and $\sigma\tau_+$ transitions have the transition from the occupied to the open orbits, the difference of the total transition strength between the $\sigma\tau_-$ and the $\sigma\tau_+$ transition is proportional to the number of the neutron excess of the parent nucleus. This is one way of demonstrating the sum rule by Gaarde et al., [Gaa80] given by

$$\sum_f |\langle f|\sum_{k=1}^{A}\sigma(k)\tau_-(k)|i\rangle|^2-\sum_f|\langle f|\sum_{k=1}^{A}\sigma(k)\tau_+(k)|i\rangle|^2$$
$$=12\langle i|T_z|i\rangle=6(N-Z)\,. \tag{2-10}$$

Equation (2-10) is actually very general and does not depend on a particular shell model. In fact, Gaarde et al. derived the sum rule from the operator identity

$$(\sigma\tau_-)^\dagger\cdot(\sigma\tau_-)-(\sigma\tau_+)^\dagger\cdot(\sigma\tau_+)=12T_z\,. \tag{2-11}$$

It is conserved in the presence of residual interactions

since the right hand side of Equation (2-10) depends only on the ground state of the parent nucleus.

Equation (2-8) and the sum rule (2-10) enable us to make a qualitative discussion about the shape of the GT strength function. Let us first consider magic nuclei such as ^{48}Ca, ^{90}Zr, and ^{208}Pb. In the case of ^{48}Ca, there is only one valence level, $f^{\nu}_{7/2}$, and we may see just two dominant peaks that come from PH excitations $f^{\pi}_{5/2}f^{\nu-1}_{7/2}$ and $f^{\pi}_{7/2}f^{\nu-1}_{7/2}$. ^{90}Zr is exactly in the same situation as ^{48}Ca by replacing the $f^{\nu}_{7/2}$ orbit with $g^{\nu}_{9/2}$. It is slightly more complicated for ^{208}Pb since it has many valence orbits like p, f, h, and i. However, h and i neutrons would play a dominant role and the strength function would still have a simple structure. [Kre81, Gaa82] The residual interaction will mix these PH excitations. (More about the GT energy systematics and the strength observed will be discussed in the following two sections.) For these magic nuclei, there exists practically no $\sigma\tau_+$ strength because all the neutron orbits possible for the transition are already occupied and the sum rule value of Equation (2-10) comes mostly from the $\sigma\tau_-$ strength.

Next, let us consider open shell nuclei, where most of the β^+ decays are observed. In these nuclei, the pairing interaction mixes the particles into the normally open levels, and the ground state of the parent nucleus can be described by occupation probabilities v^2 of each orbit. Then the transition strength given by Equation (2-5) should be

modified, in order to account for the partial occupation of levels, to

$$B(GT;j_1\ j_2)=2|\langle j_1||\sigma||j_2\rangle|^2 v_{j_1}^2 (1-v_{j_2}^2). \qquad (2\text{-}12)$$

Because of this addititonal contribution of the occupation probability to the transition strength, the PH excitation with the smaller ℓ may compete with that of the larger ℓ. Also there is a nonvanishing probability of the $\sigma\tau_+$ transition since the levels are now partially occupied, and the Pauli blocking is incomplete. The treatment of these open shell nuclei will be the subject of Chapter III.

2-2 Energy systematics

The main feature of the $\sigma\tau_-$ strength distribution recently observed by intermediate energy (p,n) reactions can be characterized by a broad peak with the width of about 4 MeV, which is known as the giant GT resonance. [And80, Bai80, Hor80, Gaa82] It has been seen next to a sharp peak known as the IAS which was found by Anderson and Wong in 1961. [And61] Since the IAS and the giant GT state almost exhaust the corresponding strength, the mean energy, defined by

$$E=\langle 0|\hat{O}^\dagger[H,\hat{O}]|0\rangle/\langle 0|\hat{O}^\dagger\hat{O}|0\rangle, \qquad (2\text{-}13)$$

which is measured from the ground state of the parent nucleus, gives an adequate estimate for the energy of the

states. [Suz82] Here $|0\rangle$ is the ground state of the parent nucleus, H is the Hamiltonian and $\hat{O}$ is Fermi or GT operator given by

$$\hat{O}= \sum_k \tau_-(k) \qquad \text{for the IAS} \tag{2-14a}$$

$$\hat{O}= \sum_k \sigma_\mu(k)\,\tau_-(k) \qquad \text{for the giant GT state.} \tag{2-14b}$$

The energy splitting between the IAS and the giant GT state can be expressed in a simple form when evaluated with Equation (2-13). Since the operators of Equations (2-14) have no spatial dependence, the energy of the giant GT state has contributions from the one-body spin-orbit interaction and residual interaction part of the Hamiltonian, and the energy of the IAS has contributions only from residual interaction part. Bertsch estimated the residual interaction part with a simple model and expressed the energy splitting as [Ber82b]

$$E_{GT}-E_{IAS}=\langle H_{so}\rangle_{GT}+ \frac{\kappa_{\sigma\tau}-\kappa_\tau}{A} B(GT;0\rightarrow GT) \tag{2-15}$$

where κ_τ and $\kappa_{\sigma\tau}$ are the strength of the isospin and the spin-isospin component of the long-range residual interaction:

$$v_{res}(1,2)= \frac{\kappa_\tau}{A}\,\tau_1\cdot\tau_2\,\frac{\kappa_{\sigma\tau}}{A}\,\sigma_1\cdot\sigma_2\,\tau_1\cdot\tau_2. \tag{2-16}$$

Horen et al. plotted Equation (2-15) for nuclei ranging from ^{90}Zr to ^{208}Pb, assuming that the mean spin-orbit energy, the

first term of Equation (2-15), is not dependent on A. [Hor81] They found the best fit to the data by

$$E_{GT}-E_{IAS}=6.7-30.0(N-Z)/A \text{ MeV}. \quad (2-17a)$$

The (N-Z) dependence of the second term can be seen from the sum rule limit of Equation (2-10). Nakayama et al. assumed that the spin-orbit energy has $A^{-1/3}$ dependence and obtained the best fit given by [Nak82]

$$E_{GT}-E_{IAS}=26.0A^{-1/3}-18.5(N-Z)/A \text{ MeV}. \quad (2-17b)$$

To study this in more detail, the GT strength function has been investigated within the framework of the PH-RPA. For example, Bertsch et al. have used the Tamm-Dancoff approximation (TDA) with a zero-range interaction of the Landau-Migdal type: [Ber81a]

$$V_{\sigma\tau}\sigma_1\cdot\sigma_2\tau_1\cdot\tau_2\delta(r_1-r_2). \quad (2-18)$$

The energy of the giant GT state in the whole range of medium heavy nuclei was reproduced within one MeV with the interaction strength

$$V_{\sigma\tau}=220 \text{ MeV fm}^3 \quad (2-19a)$$

for a model in which single particle energies were calculated from a WS potential and

$$V_{\sigma\tau}=200 \text{ MeV fm}^3 \quad (2-19b)$$

for the Hartree-Fock (HF) single particle model with the Skyrme III interaction. They also found about 20% of the strength at low excitation energy, which accords with the experiment. [And80, Bai80] Speth et al. have generalized the Landau-Migdal interaction by including the one-pion and one-rho-exchange potential given by

$$-f_\pi^2 m_\pi [h_2^{(1)}(im_\pi r)\exp(-m_\pi r) S_{12}(\hat{r}) + \frac{1}{3}\sigma_1\cdot\sigma_2 \exp(-m_\pi r)/m_\pi r]\tau_1\cdot\tau_2$$

$$+f_\rho^2 m_\rho [h_2^{(1)}(im_\rho r)\exp(-m_\rho r) S_{12}(\hat{r}) - \frac{2}{3}\sigma_1\cdot\sigma_2 \exp(-m_\rho r)/m_\rho r]\tau_1\cdot\tau_2 \quad (2\text{-}20)$$

explicitly in addition to the zero-range part (2-18) in order to correct for the finite range of the nucleon-nucleon interaction. [Spe80, Kre81]

There has been another approach to the problem, namely the FSM calculation. [McG80] Instead of assuming a functional form for two-body interactions, the FSM treats them as parameters and fit them to the measured low-lying states. However, its application is restricted to the lighter nuclei due to the dimensions involved. Recent calculations for fp shell nuclei gave good agreement to the excitation energy but required uniform reduction of strength for the states observed. [Goo81, McG81]

In summary, the energy of the main peak in the GT strength distribution can be reproduced without much difficulty by applying various theories. However, as will be discussed in the next section, though the theory gives

reasonable agreement with the shape of the strength function, the total strength observed is far less than that predicted by the sum rule limit of Equation (2-10).

2-3 Empirical strength reduction

As discussed before, there is a sum rule for the GT transition. For nuclei with a large neutron excess, the $\sigma\tau_+$ strength is negligible and the total $\sigma\tau_-$ strength has upper limit of 6(N-Z) given by Equation (2-10). But the strength actually observed is only a small fraction of the limit. In fact, the quenching phenomena has been observed across the board for the spin dependent transitions. According to Bertsch, "perhaps the main suprise now is that the quenching has not shown up more obviously in the magnetic moment". [Ber82b]

Many explanations for the quenching have been proposed such as the excitation of nucleons into Δ-isobar states, [Ose79, Ber81b, Bro81, Boh81, Har81, Ost82] and more complicated configurations like two-particle two-hole excitations at high excitation energies. [Ber82a] But any single theory has not been able to account for all the quenching observed.

In this thesis, however, it is not our main purpose to devise a theory to explain the quenching mechanism. But we want to know the percentage which should be explained beyond the current model space, since we may assume that the

Table 1 Empirical strength reduction

Nucleus	Transition	Quenching factor†	Reference
^{26}Mg	GT	1.6	Blo81
^{42}Ca	GT	1.9	Goo81
	M1	3.1	McG81
^{48}Ca	GT	4.2	Ost81
	M1	2.2	McG81
^{90}Zr	M1	3.9	Ana82
^{208}Pb	GT	2.0	Kre81

†Defined in the text by Equation (2-21).

$\sigma\tau_+$ strength is quenched in a similar manner.

In Table 1, we collected calculations for the GT and the M1 transitions. The quenching factor of the third column is defined by the ratio,

Quenching factor

=(Theoretical strength)/(Strength observed). (2-21)

The theory used is either the PH-RPA or the shell model calculation which does not include any mesonic effects or more complicated configurations. Note that in most references the quenching is defined with respect to the sum rule limit 6(N-Z) for the GT transition or to the unperturbed limit for the M1 transition. Instead, in Equation (2-21) the theoretical strength is the strength which can actually be obtained from the shell model description. Therefore, the quenching factor of Equation (2-21) represents a factor which must be explained from contributions beyond the shell

model space to reproduce the data. We observe from Table 1 that the quenching factor is anywhere between 2∿4. However, we should not attempt to find any correlation from Table 1 such as between the quenching factor and the size of nuclei since independent theories have been used for each nucleus.

Chapter III

FORMALISM

3-1 Introduction

In this chapter, we shall develop the QP-RPA for PH states of unlike nucleons. This will be applied to the GT β^+ decay in medium heavy nuclei with a large neutron excess. No other experimental evidence is yet available for the $\sigma\tau_+$ mode except a recent (n,p) experiment on light nuclei such as ^{6}Li, ^{12}C, and ^{28}Si by Brady and his co-workers. [Bra82]

We need to describe the β^+ decays by QP's since most of the β^+ decays of medium heavy nuclei are observed from open shell nuclei. New features in the QP theory compared to the PH theory are the partial occupation of single particle levels and the particle-particle (PP) interaction between QP's. The role of the partial occupation of the levels was discussed in the last chapter. The PP interaction is attractive while the PH interaction is repulsive in the spin-flip and isospin-flip transition. Therefore, the transition can be observed as a decay process only when the attractive PP interaction is more dominant than the PH interaction, since otherwise the final state would be located too high above the Q-window. Also, we find another evidence of the importance of the PP interaction from the

recent (p,n) experiments on calcium isotopes. [And80, Goo81] For ^{48}Ca, only the PH states are possible since the $f^{\nu}_{7/2}$ orbit is fully occupied, and it is observed that more than 80% of the strength is at the higher state which is mostly two-QP excitation of $f^{\pi}_{5/2}f^{\nu-1}_{7/2}$. On the other hand, for ^{42}Ca, the states are chiefly of PP character and only the lowest state, which is mostly $f^{\pi}_{7/2}f^{\nu-1}_{7/2}$, is observed depleting all the strength. Toki and Bertsch suggested that the GT strength moves up gradually from the lowest state to the higher state as the neutron number is increased. [Tok82]

3-2 Single particle wavefunctions

It is desirable to use a self-consistent formalism such as the Hartree-Fock-Bogolyubov calculation for a description of the initial ground state. But it was shown in the calculation by Bertsch et al. [Ber81a] that the self-consistent treatment did not introduce any notable improvement on the GT energy systematics. Therefore, we use the BCS theory based on a simple one-body potential such as a WS potential. We take a pairing interaction between like nucleons only. Sandhu and Rustgi investigated neutron-proton pairing for even-even N≠Z isotopes. [San76] Their results show that for nuclei $(N-Z)>2$ the neutron-proton pairing correlations are completely absent.

We use a pairing interaction given by [Lan64, p12]

$$\langle (j_1,j_2)J|v_{pair}|(j_3,j_4)J\rangle = -\tfrac{1}{2}G\delta_{J,0}\sqrt{(2j_1+1)(2j_3+1)} \qquad (3\text{-}1)$$

where G is the strength of the interaction. Given the interaction, the BCS ground state is specified by the QP energies E_j and the occupation amplitudes v_j associated with single particle orbits. E_j and v_j are determined by solving the BCS equations given by Equations (A-3) simultaneously. The derivation of the BCS theory can be found in many textbooks. [Lan64, Fet71, Law80] In Appendix A, we introduce the BCS equations and show how to solve them iteratively.

3-3 Quasi-particle random phase approximation

The application of the QP-RPA to nuclear physics was started by Baranger, who studied the low-lying states in even-even spherical nuclei. [Bar60] It is straightforward to extend his formalism to one for the PH states of unlike nucleons.

The initial state is 0^+ ground state of an even-even nucleus. In the BCS theory, this ground state is a vacuum for QP's. Then the $\sigma\tau_\pm$ transition creates two-QP excitations in the odd-odd nucleus isobarically adjacent to the parent nucleus. The final eigenstate is obtained by diagonalizing the Hamiltonian in the space of the two-QP excitations.

We define three interaction matrices G, F, and H which are coupled to J in the two-QP space as

$$G^J_{j_1 j_2, j_3 j_4} = \langle [j_1(1) j_2(2)]J | v_{res}(1,2) | [j_3(1) j_4(2)]J \rangle \qquad (3\text{-}2)$$

$$F^J_{j_1j_2,j_3j_4}=\langle[j_1(1)j_2(1)^{-1}]J|v_{res}(1,2)|[j_3(2)j_4(2)^{-1}]J\rangle \quad (3\text{-}3)$$

$$H^J_{j_1j_2,j_3j_4}=\langle[j_1(1)j_2(2)^{-1}]J|v_{res}(1,2)|[j_3(1)j_4(2)^{-1}]J\rangle \quad (3\text{-}4)$$

where v_{res} denotes the two-body residual interaction which shall be specified by a model later on. G and F are the usual PP and PH interaction energies respectively and H is the exchange term of F as shown in Figure 2, (a), (b), and (c) respectively. They all satisfy the following symmetry relations:

$$\begin{aligned} G_{j_1j_2,j_3j_4} &= G_{j_3j_4,j_1j_2} \\ &= G_{j_2j_1,j_4j_3}(-1)^{j_1+j_2+j_3+j_4} \\ &= G_{j_4j_3,j_2j_1}(-1)^{j_1+j_2+j_3+j_4}. \end{aligned} \quad (3\text{-}5)$$

The two-QP states are not antisymmetrized because they consist of neutron-proton pairs. But we keep a convention that j_1 and j_3 always denote neutron (proton) states while j_2 and j_4 always denote proton (neutron) states for the $\sigma\tau_+$ ($\sigma\tau_-$) transition.

The B-th eigenstate (x_B,y_B), where x and y are vectors in the two-QP space, with an excitation energy ω_B measured from the RPA ground state satisfies the RPA eigenvalue equation, [Bar60, Row68, Lan80]

$$\omega_B \begin{pmatrix} x_B \\ y_B \end{pmatrix} = \begin{pmatrix} D+P & R \\ -R & -D-P \end{pmatrix} \begin{pmatrix} x_B \\ y_B \end{pmatrix}, \quad (3\text{-}6)$$

Figure 2 Elements of interaction matrices, (a) G, (b) F, and (c) H

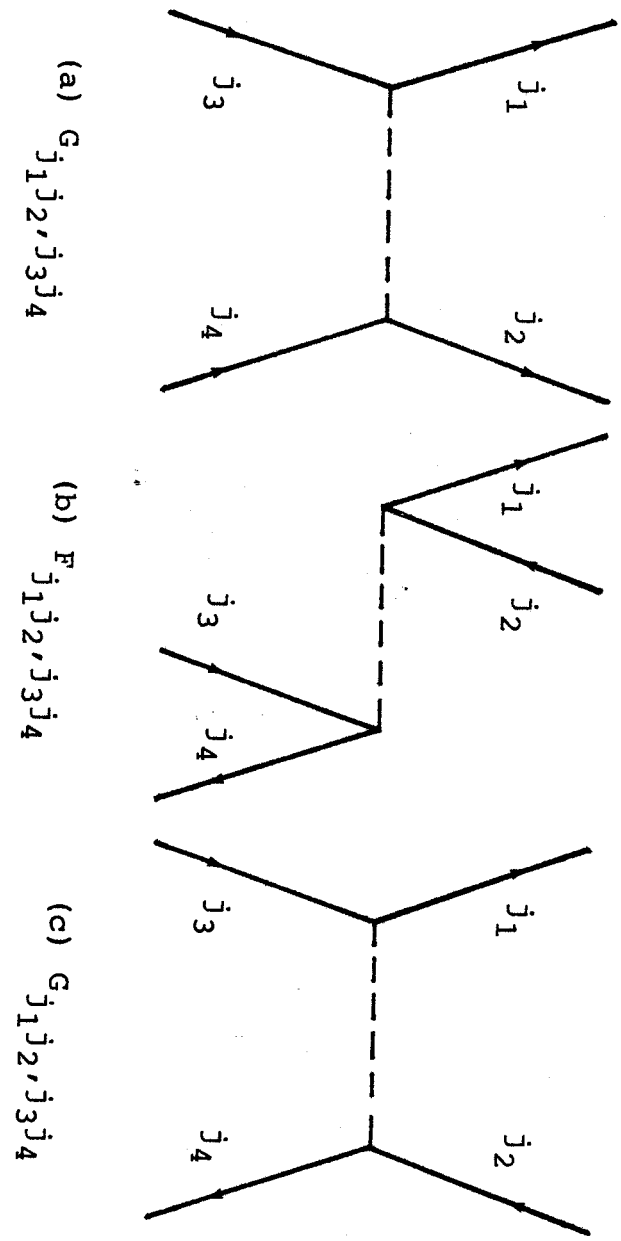

where D is a diagonal matrix of the unperturbed two-QP energies given by

$$D_{j_1j_2,j_3j_4}=(E_{j_1}+E_{j_2})\delta_{j_1j_2,j_3j_4}, \tag{3-7}$$

and matrices P and R are expressed by G, F, and H as

$$\begin{aligned}P_{j_1j_2,j_3j_4}&=G_{j_1j_2,j_3j_4}(u_{j_1}u_{j_2}u_{j_3}u_{j_4}+v_{j_1}v_{j_2}v_{j_3}v_{j_4})\\&+(F_{j_1j_2,j_3j_4}-H_{j_1j_2,j_3j_4})(u_{j_1}v_{j_2}u_{j_3}v_{j_4}+v_{j_1}u_{j_2}v_{j_3}u_{j4})\end{aligned} \tag{3-8}$$

$$\begin{aligned}R_{j_1j_2,j_3j_4}&=-G_{j_1j_2,j_3j_4}(u_{j_1}u_{j_2}v_{j_3}v_{j_4}+v_{j_1}v_{j_2}u_{j_3}u_{j_4})\\&+(F_{j_1j_2,j_3j_4}-H_{j_1j_2,j_3j_4})(u_{j_1}v_{j_2}v_{j_3}u_{j_4}+v_{j_1}u_{j_2}u_{j_3}v_{j_4})\end{aligned} \tag{3-9}$$

where u is defined by

$$u=\sqrt{1-v^2}\ . \tag{3-10}$$

Since the interaction between two QP's takes place in a residual nucleus, we should calculate E's, u's, and v's, which appear in Equations (3-7)∿(3-9), in the daughter nucleus. The u's and v's in the daughter nucleus are determined under the constraint (see Equation (A-3b))

$$\sum_{k}^{\text{Neutrons(Protons)}}(2j_k+1)v_{j_k}^2=N\pm1\ \ (Z\mp1) \tag{3-11}$$

where N and Z are the number of neutrons and protons respectively in the parent nucleus, and the upper (lower) sign is for the $\sigma\tau_+$ ($\sigma\tau_-$) transition. The constraint (3-11)

determines the average mass of the ground state of the daughter nucleus, represented by the lowest two-QP state, to be equal to (N+Z). [Law80, p359]

The GT transition strength B(GT) to the B-th eigenstate can be expressed by

$$B(GT;0\to B)=(f^{\dagger},g^{\dagger})\begin{pmatrix}x_B\\ y_B\end{pmatrix}(x_B{}^{\dagger},y_B{}^{\dagger})\begin{pmatrix}f\\ g\end{pmatrix}, \tag{3-12}$$

where vectors f and g are forward and backward GT transition amplitudes respectively and given by

$$f_{j_1j_2}=\langle j_1||\sigma\tau_{\pm}||j_2\rangle\hat{u}_{j_1}\hat{v}_{j_2} \tag{3-13}$$

$$g_{j_1j_2}=\langle j_1||\sigma\tau_{\pm}||j_2\rangle\hat{v}_{j_1}\hat{u}_{j_2}. \tag{3-14}$$

A hat on top of u and v means that they are calculated in the parent nucleus. (Remember that we calculated them in the daughter nucleus to find interaction energies G, F, and H, Equations (3-2)∿(3-4).) The reduced matrix element in Equation (3-13) or (3-14) becomes,

$$\langle j_1||\sigma\tau_{\pm}||j_2\rangle=-\sqrt{2}\int\psi_{j_1}(r)\psi_{j_2}(r)r^2dr\ \sqrt{(2j_1+1)(2j_2+1)}$$
$$\times\left\{\frac{1}{\sqrt{3}}\langle j_1\tfrac{1}{2}j_2-\tfrac{1}{2}|10\rangle(-1)^{j_1+\frac{1}{2}}+\frac{\sqrt{2}}{\sqrt{3}}\langle j_1\tfrac{1}{2}j_2\tfrac{1}{2}|11\rangle(-1)^{j_1+j_2+\ell_1}\right\} \tag{3-15}$$

where $\psi_j(r)$ is the radial wavefunction of the orbit j.

3-4 Remarks

It is easy to see by direct substitution that eigenvalues of Equation (3-6) come in pairs as $\pm|\omega|$. The eigenvector of the negative energy is obtained by interchanging x and y of the eigenvector of the corresponding positive energy. For the non-charge-exchange transition, the negative energy solution has no physical meaning because it is lower than the ground state in energy. For the charge-exchange transition, we still take the positive energy solution only. The negative energy solution represents the backward transition, namely when we treat the $\sigma\tau_+$ ($\sigma\tau_-$) transition, the negative energy solution will provide a solution for the $\sigma\tau_-$ ($\sigma\tau_+$) transition.

The eigen energy ω obtained by Equation (3-6) is calculated with respect to the ground state of the parent nucleus. Since the final state of the charge-exchange transition appears in a nucleus different from the parent nucleus, it is not easy to find the excitation energy with respect to the ground state of the daughter nucleus, and we do not try it here.

In the case of the PH-RPA, the number of PH excitations for the forward transition differs from that for the backward transition as can be seen from Figure 1. Here the the energies do not appear in pairs as they did earlier. [Aue81] But if one treats the PH-RPA as a limiting case of the QP-RPA, then the energies come in pairs again since the

numbers of the two-QP excitations for the forward and backward are the same, though some of the states have no transition strength.

Chapter IV

DETAILS OF CALCULATION

4-1 One- and two-body interaction

We have performed BCS calculations for protons and neutrons seperately, taking approximately two harmonic oscillator shells around the Fermi sea as a model space. Single particle wavefunctions are from a WS well,

$$V(r)=V_0F(r) \tag{4-1}$$

where

$$F(r)=1/\left[1+\exp\{(r-r_0)/a\}\right]. \tag{4-2}$$

We use the standard parameters:

$$V_0=50 \text{ MeV}, \; r_0=1.28 \text{ fm}, \; a=0.65 \text{ fm}. \tag{4-3}$$

The spin-orbit energy V_{so} is later calculated with the above single particle wavefunctions $\psi_j(r)$ by

$$V_{so}=W_{so}\int |\psi_j(r)|^2 \frac{1}{r} [dF(r)/dr] \; r^2dr. \tag{4-4}$$

We used the parameters determined by low-energy elastic proton scattering by Becchetti and Greenless: [Bec69]

$$W_{so}=6.2 \text{ MeV}, \; r_{so}=1.01 \text{ fm}, \; a_{so}=0.75 \text{ fm}. \tag{4-5}$$

Table 2 Energy gap and strength of the particle-particle interaction

Nucleus	Energy gap (MeV)		V_{pp} (MeV fm^3)
	Neutrons	Protons	
^{102}Cd	0.94	1.02	482
^{104}Cd	1.03	0.99	495
^{108}Sn	1.39	0.00	517
^{110}Sn	1.40	0.00	517
^{116}Te	1.61	1.17	510
^{118}Te	1.60	1.14	510
^{120}Xe	1.56	1.44	468
^{122}Xe	1.54	1.41	489
^{126}Ba	1.49	1.54	463
^{128}Ba	1.48	1.51	475
^{132}Ce	1.38	1.55	472
^{134}Ce	1.28	1.52	490
^{136}Nd	1.25	1.54	474
^{138}Nd	1.08	1.43	490
^{140}Nd	0.81	1.47	531

The same pairing strength G of Equation (3-1) given by

$$G=22.7/A \text{ MeV for neutrons, } 28.4/A \text{ MeV for protons} \qquad (4\text{-}6)$$

has been used for all the nuclei we have treated. We first adjusted the pairing strength to reproduce the empirical energy gap Δ found by the binding energy systematics and then averaged over all the nuclei for neutrons and protons seperately. The energy gap obtained by using the pairing strength given by Equation (4-6) are tabulated in Table 2.

As for a residual two-body interaction, we use only

the central part of the interaction in the zero-range approximation,

$$v_{res}(1,2)=\{V_{oo}+V_{\sigma\tau}\ \sigma_1\cdot\sigma_2\ \tau_1\cdot\tau_2\}\ \delta(r_1-r_2). \tag{4-7}$$

Matrix elements of the δ-function interaction can be expressed analytically as presented in Appendix B. If one considers only the unnatural parity states as the GT states, then the interaction matrices G and (F-H) of Equations (3-2)$\sim$(3-4) can be written from the results of Appendix B as

$$\begin{aligned} G^J_{j_1j_2,j_3j_4} &= -V_{pp}\langle[j_1(1)j_2(2)]J|\delta(r_1-r_2)|[j_3(1)j_4(2)]J\rangle \\ &= -\frac{V_{pp}}{4\pi}\frac{\sqrt{(2j_1+1)(2j_2+1)(2j_3+1)(2j_4+1)}}{2J+1} \\ &\times\int\psi_{j_1}(r)\psi_{j_2}(r)\psi_{j_3}(r)\psi_{j_4}(r)r^2dr\times\Big\{\langle j_1\tfrac{1}{2}j_2-\tfrac{1}{2}|J0\rangle\langle j_3\tfrac{1}{2}j_4-\tfrac{1}{2}|J0\rangle \\ &\times(-1)^{j_1+j_3+\ell_1+\ell_3-1}+\langle j_1\tfrac{1}{2}j_2\tfrac{1}{2}|J1\rangle\langle j_3\tfrac{1}{2}j_4\tfrac{1}{2}|J1\rangle(-1)^{j_1+j_2+j_3+j_4}\Big\} \end{aligned} \tag{4-8}$$

$$\begin{aligned} &F^J_{j_1j_2,j_3j_4}-H^J_{j_1j_2,j_3j_4} \\ &=V_{ph}\langle[j_1(1)j_2(1)^{-1}]J|\sigma_1\cdot\sigma_2\ \tau_1\cdot\tau_2\ \delta(r_1-r_2)|[j_3(2)j_4(2)^{-1}]J\rangle \\ &=\frac{V_{ph}}{\pi}\frac{\sqrt{(2j_1+1)(2j_2+1)(2j_3+1)(2j_4+1)}}{2J+1} \\ &\times\int\psi_{j_1}(r)\psi_{j_2}(r)\psi_{j_3}(r)\psi_{j_4}(r)r^2dr\times\Big\{\langle j_1\tfrac{1}{2}j_2-\tfrac{1}{2}|J0\rangle\langle j_3\tfrac{1}{2}j_4-\tfrac{1}{2}|J0\rangle \\ &\times(-1)^{j_1+j_3-1}+\langle j_1\tfrac{1}{2}j_2\tfrac{1}{2}|J1\rangle\langle j_3\tfrac{1}{2}j_4\tfrac{1}{2}|J1\rangle(-1)^{j_1+j_2+j_3+j_4+\ell_1+\ell_3}\Big\}. \end{aligned} \tag{4-9}$$

Equations (4-8) and (4-9) are equivalent to taking the residual interaction given by Equation (4-7). Relations

between the two sets of coefficients are:

$$V_{pp}=V_{\sigma\tau}-V_{oo} \tag{4-10a}$$

$$V_{ph}=(3V_{\sigma\tau}-V_{oo})/4. \tag{4-10b}$$

The strength of the PP interaction depends on the size of the two-QP space. This can be seen from the energy shift in the perturbation theory,

$$\Delta\omega_{j_1j_2}=P_{j_1j_2,j_3j_4} + \sum_{j_3j_4\neq j_1j_2} \frac{\left[P_{j_1j_2,j_3j_4}\right]^2}{E_{j_1}+E_{j_2}-E_{j_3}-E_{j_4}} + \sum_{j_3j_4} \frac{\left[R_{j_1j_2,j_3j_4}\right]^2}{E_{j_1}+E_{j_2}+E_{j_3}+E_{j_4}}. \tag{4-11}$$

The number of the PH states is restricted while that of the PP states is not. For the high-lying PH states, the interaction matrix elements are very small since the radial quantum numbers of the particle and the hole states are different. Therefore, the contribution of the PH states to the sums in Equation (4-11) has the upper limit. Contrary to this, the number of the PP states is not restricted as well as their radial quantum numbers can be the same, and the coherent contribution to the sums can be large. Although this is of the second order in the perturbation theory, we found that it is necessary to introduce a significant variation in V_{pp} when the size of the model space is changed. In this calculation, we take a model space which consists of unperturbed two-QP states whose energy is less

Figure 3 Schematic description of the particle-particle interaction energy in ^{42}Sc

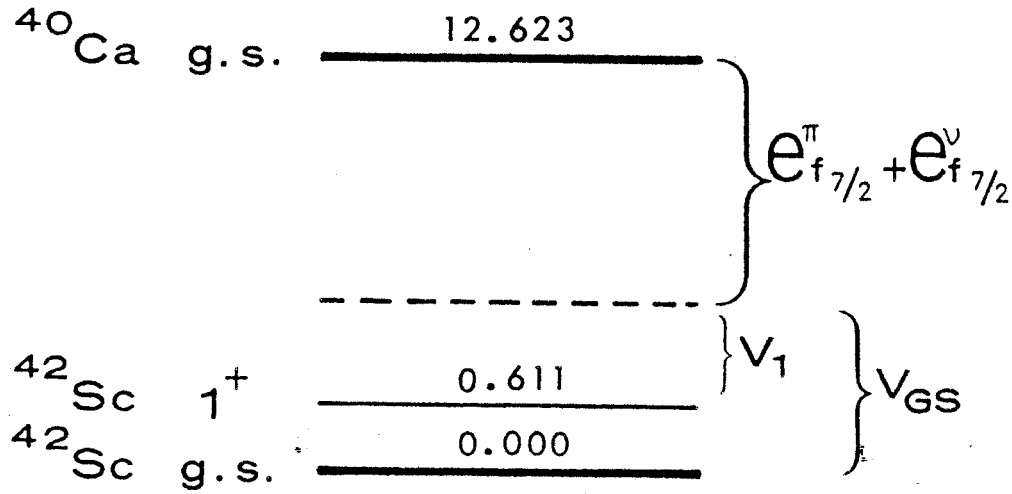

than 15 MeV. Using such a model space, we achieve more than 99% of the sum rule given by Euqation (2-10) for all the nuclei we have treated, except tin isotopes which show 93% of the sum rule.

We use the strength of the PH interaction given by Equation (2-19a) which has been obtained by reproducing the giant GT states. We determine the strength of the PP interaction from the lowest 1^+ state in ^{42}Sc. The residual interactions V_{GS} and V_1, in the ground state and in the 1^+ state respectively, as shown in Figure 3, can be found empirically

by

$$V_{GS}=BE(^{42}Sc)-BE(^{40}Ca)-\{e^{\pi}_{f_{7/2}}+e^{\nu}_{f_{7/2}}\}$$

$$=BE(^{42}Sc)+BE(^{40}Ca)-BE(^{41}Sc)-BE(^{41}Ca)=-3.17\ \text{MeV} \qquad (4\text{-}12a)$$

$$V_1=V_{GS}-(-0.61)=-2.56\ \text{MeV} \qquad (4\text{-}12b)$$

where we used binding energies from the atomic mass table by Wapstra and Gove. [Wap71] We find that

$$V_{pp}=1100\ \text{MeV fm}^3 \qquad (4\text{-}13)$$

is required to reproduce V_1 using a single configuration in the two-QP space. Then we take into account the effect of the larger model space by first calculating the energy of the lowest 1^+ state for each nucleus with only one two-QP state. Next, we adjust V_{pp} to get the same energy when using the larger model space. The V_{pp}'s determined, then, is from 460 to 530 Mev fm^3 for the nuclei we have treated. They are tabulated in the last column of Table 2.

4-2 Excitation energy and transition rate

We solve the RPA eigenvalue equation, given by Equation (3-6), by two equivalent schemes, a direct diagonalization of the Hamiltonian and a Green's function method. We used an algorithm for the diagonalization described by Bertsch. [Ber82b] Since the Hamiltonian matrix is not symmetric, the usual Householder method can not be

applied directly. While the direct diagonalization has an advantage of obtaining eigenvectors explicitly, the Green's function method gives the strength function explicitly.

To apply the Green's function method, let us define an unperturbed Green's function $G_o(\omega)$ which is a matrix in the two-QP space as

$$G_o(\omega) = \begin{pmatrix} 1/(D-\omega-i\varepsilon) & 0 \\ 0 & 1/(D+\omega-i\varepsilon) \end{pmatrix} , \qquad (4\text{-}14)$$

where D is given by Equation (3-7). Then it can be shown that the Green's function $G(\omega)$ is expressed as [Tsa78]

$$G(\omega) = [1+G_o(\omega)\upsilon]^{-1} G_o(\omega) , \qquad (4\text{-}15)$$

where

$$\upsilon = \begin{pmatrix} P & R \\ R & P \end{pmatrix} \qquad (4\text{-}16)$$

with P and R defined by Equations (3-8) and (3-9) respectively. The GT strength function $S_{GT}(\omega)$, which is defined by

$$S_{GT}(\omega) = \sum_B |\langle B|\sigma\tau_{\pm}|0\rangle|^2 \, \delta(\omega_B-\omega) , \qquad (4\text{-}17)$$

is expressed in terms of the Green's function as [Ber75]

$$S_{GT}(\omega) = \frac{1}{\pi} (f^{\dagger}, g^{\dagger}) \, \mathrm{Im}[G(\omega)] \begin{pmatrix} f \\ g \end{pmatrix} , \qquad (4\text{-}18)$$

where f and g are the forward and backward transition

amplitudes defined by Equations (3-13) and (3-14) respectively. Finally, log(ft) values were calculated by Equation (2-6) from the transition strength using

$$D/(g_A/g_V)^2=4140 \text{ sec} \qquad (4\text{-}19)$$

for the constant that appears in Equation (2-6).

Chapter V

APPLICATION TO β^+ DECAY IN MEDIUM HEAVY EVEN-EVEN NUCLEI

5-1 Experimental data

As an application to the QP-RPA on the $\sigma\tau_+$ strength we collected nuclei which are β^+ unstable from the "Table of Isotopes", seventh edition by Lederer et al. [Led78] We choose only even-even nuclei because they have 0^+ ground state and the calculation is simple. We can find fifteen nuclei between mass numbers A=100∿150. When there are more than two final states in the data table, we choose the one which has the smallest log(ft) value to compare with the theory. These nuclei are given in Table 3.

5-2 Results of the theory

To see the effect of the various approximation, we have performed calculations with no residual interaction, with the PH interaction only, and with both the PH and PP interactions. The QP-TDA calculations have also been done by setting R=0 in Equation (3-6). The theory is compared with the data in Table 3 and Figure 4.

The unperturbed results (with no residual interaction) predict the strength which is 30 times or more

Table 3 Log(ft) values of β^+ decay

Nucleus	QP-TDA			QP-RPA			Exp.	Quenching factor[†]
	No int.	PH int. only	PP+PH int.	PH int. only	PP+PH int.			
^{102}Cd	2.52	2.55	2.53	2.75	3.01		4.0	9.8
^{104}Cd	2.58	2.60	2.59	2.83	3.13		4.2	11.6
^{108}Sn	2.58	2.59	2.60	2.78	3.00		3.6	4.0
^{110}Sn	2.68	2.69	2.70	2.90	3.06		3.4	2.2
^{116}Te	3.55	3.88	3.72	4.10	4.68		4.8	1.3
^{118}Te	3.62	3.92	3.82	4.18	4.86		5.1	1.7
^{120}Xe	3.35	3.65	3.56	3.93	4.32		5.0	4.8
^{122}Xe	3.44	3.73	3.67	4.05	4.29		5.5	16.3
^{126}Ba	3.40	3.67	3.67	4.00	4.12		4.8	4.8
^{128}Ba	3.50	3.76	3.78	4.12	4.23		5.1	7.4
^{132}Ce	3.51	3.76	3.85	4.12	4.24		5.0	5.8
^{134}Ce	3.65	3.90	3.95	4.27	4.43		5.5	11.7
^{136}Nd	3.56	3.80	3.95	4.14	4.30		5.0	5.1
^{138}Nd	3.74	3.96	4.02	4.31	4.53		5.1	3.7
^{140}Nd	4.05	4.27	4.30	4.56	4.79		5.5	5.1
					Reciprocal average[††]			4.0

[†] Defined by Equation (2-21).

[††] Defined by $\tilde{r} = \dfrac{1}{\frac{1}{n}\sum_{i=1}^{n}\frac{1}{r_i}}$

Figure 4 Log(ft) values of the β^+ decay in even-even nuclei between A=100∿150

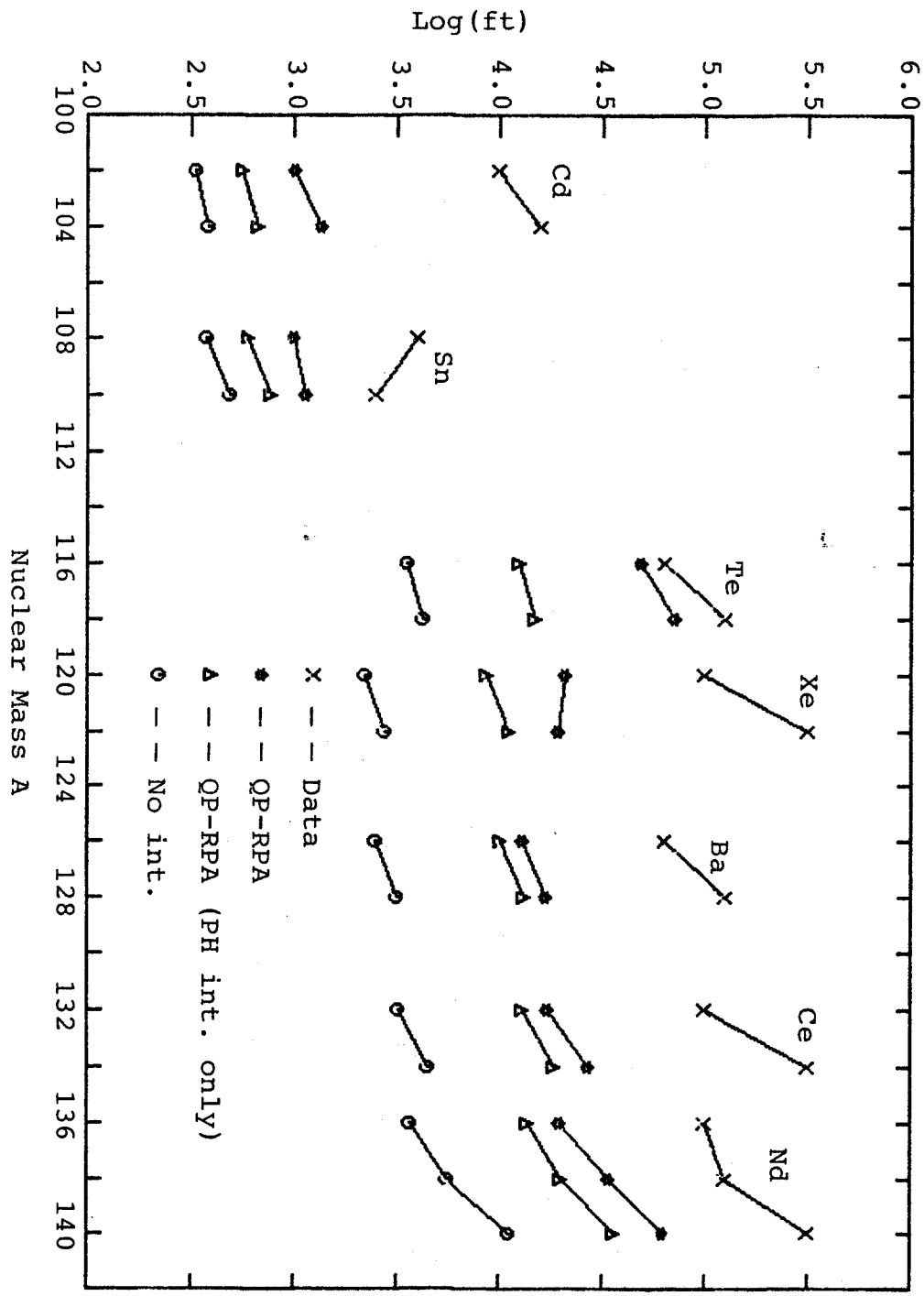

larger than what have been measured. We can observe in Figure 4 that the unperturbed results, which come solely from the pairing correlations, reproduce the general feature of isotope dependence of log(ft) values, as has been shown by Kisslinger and Sorensen. [Kis63] By comparing the unperturbed results with those of the QP-TDA from Table 3, we find that not much change is introduced by the TDA. But as can be seen from the results of the QP-RPA in Table 3 and Figure 4, the ground state correlation reduces the unperturbed strength by a factor of about 10 or more. (The role of the PH and PP interactions in the QP-RPA will be discussed in detail later in this section.) We find, in general, the QP-RPA overestimates the data significantly. This confirms that the quenching observed in other spin-flip and isospin-flip transitions is also present in the $\sigma\tau_+$ transition. The quenching factor of the QP-RPA is calculated in the last column of Table 3 by Equation (2-21). It ranges from 1.3 to 16.3 with a reciprocal average of 4.0.

To see the effects of the ground state correlation due to the residual interaction, we calculated the total $\sigma\tau_+$ strength and presented it in Table 4. Because the TDA conserves the total strength, we listed only the results of the unperturbed and the QP-RPA calculations. We find that the unperturbed sum is already reduced by a factor of almost two when only the PH interaction is applied. This is in accord with a recent calculation on ^{60}Ni by Auerbach et al.

Table 4 Total $\sigma\tau_+$ strength† and percentage of the strength above the Q-window

Nucleus	No int.	QP-RPA		Above Q (%)
		PH int. only	PP+PH int.	
^{102}Cd	25.64	15.62	12.10	33
^{104}Cd	22.54	13.04	9.37	35
^{108}Sn	22.61	14.63	12.95	36
^{110}Sn	17.78	11.37	10.48	31
^{116}Te	15.22	8.64	7.08	98
^{118}Te	11.69	6.43	5.76	98
^{120}Xe	15.29	8.14	7.51	94
^{122}Xe	12.19	6.23	6.39	93
^{126}Ba	12.43	6.17	6.96	91
^{128}Ba	10.23	4.98	6.10	92
^{132}Ce	10.33	5.04	6.37	92
^{134}Ce	8.39	4.05	5.48	94
^{136}Nd	10.17	5.07	6.52	94
^{138}Nd	7.67	3.82	5.43	95
^{140}Nd	6.01	3.23	5.30	97

†The strength is normalized to 6 for the decay of an isolated proton.

[Aue82] But when the PP interaction is added to the PH interaction, we do not find much systematic change of the total strength. Instead, a dominant state is fragmented into several weaker states and part of the strength at a lower excitation energy is transferred to a higher excitation region and consequently the β^+ decay rate is further reduced.

We can observe an interesting feature from Figure 4 that the data and the theory together can be divided into two groups, such as the first group including the first two

isotopes, cadmium and tin, and the second group with all the other isotopes collected. The transition rate of the first group is about one order of magnitude larger than that of the second group. This can be explained by the ground state configuration of protons of the parent nucleus. The first group has protons up to the Z=50 major shell and the second group has protons above the major shell.

To study this in more detail, we calculated the strength function by Equation (4-18) and plotted it in Figure 5 for three cases such as the unperturbed, the QP-RPA with the PH interaction only, and with both the PH and PP interactions. The excitation energy plotted is from the RPA ground state of the parent nucleus. Due to the reasons mentioned earlier in Section 3-3, we did not calculate the excitation energy with respect to the residual nucleus. Instead, we determine roughly the locations of the ground state and the Q-window in the daughter nucleus by comparing the theory with the measured β^+ decay spectrum. They are indicated by arrows in Figure 5 for the results of the QP-RPA. For the results with no interaction, we identified dominant unperturbed two-QP excitations by labelling them in the figure. Since the transition amplitude given by Equation (3-13) or (3-14) is larger for a transition between levels with larger ℓ, and $g^{\pi}_{9/2}$ is the highest j proton orbit for nuclei with $Z \leq 50$, $g^{\pi}_{9/2} g^{\nu}_{7/2}$ is the most dominant unperturbed configuration for the first half of nuclei we have treated.

Figure 5 $\sigma\tau_+$ strength distribution

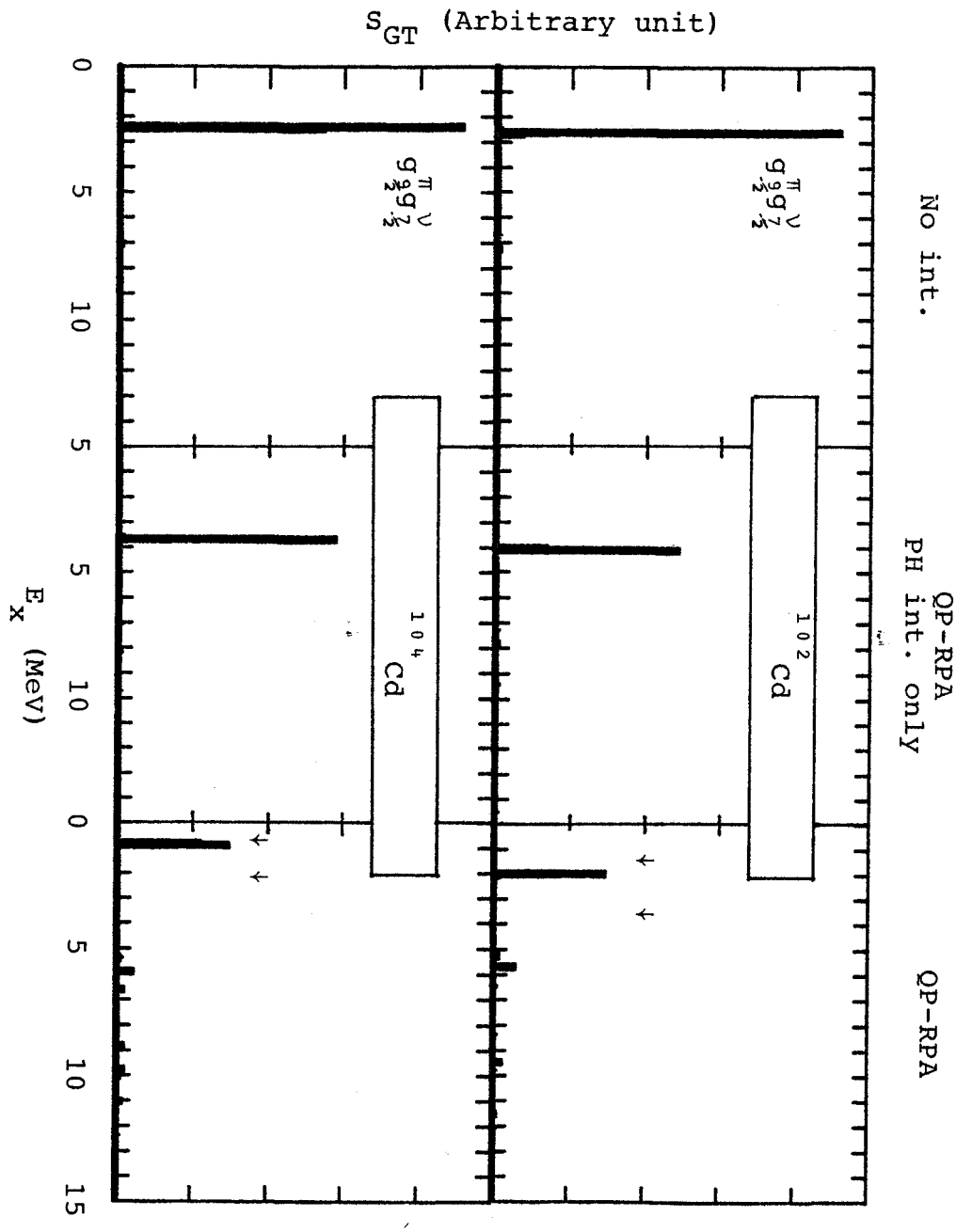

Figure 5 - Continued

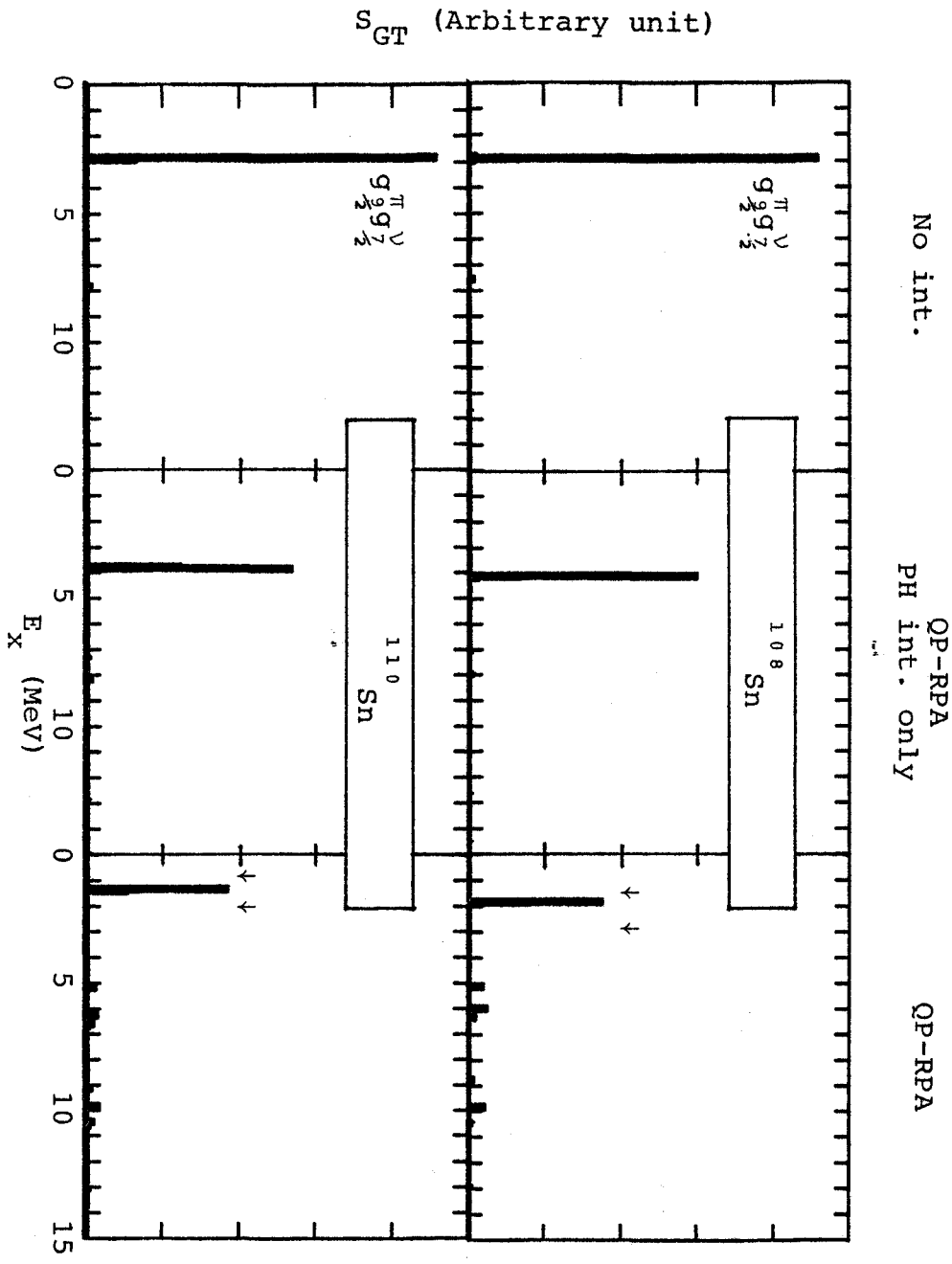

Figure 5 - Continued

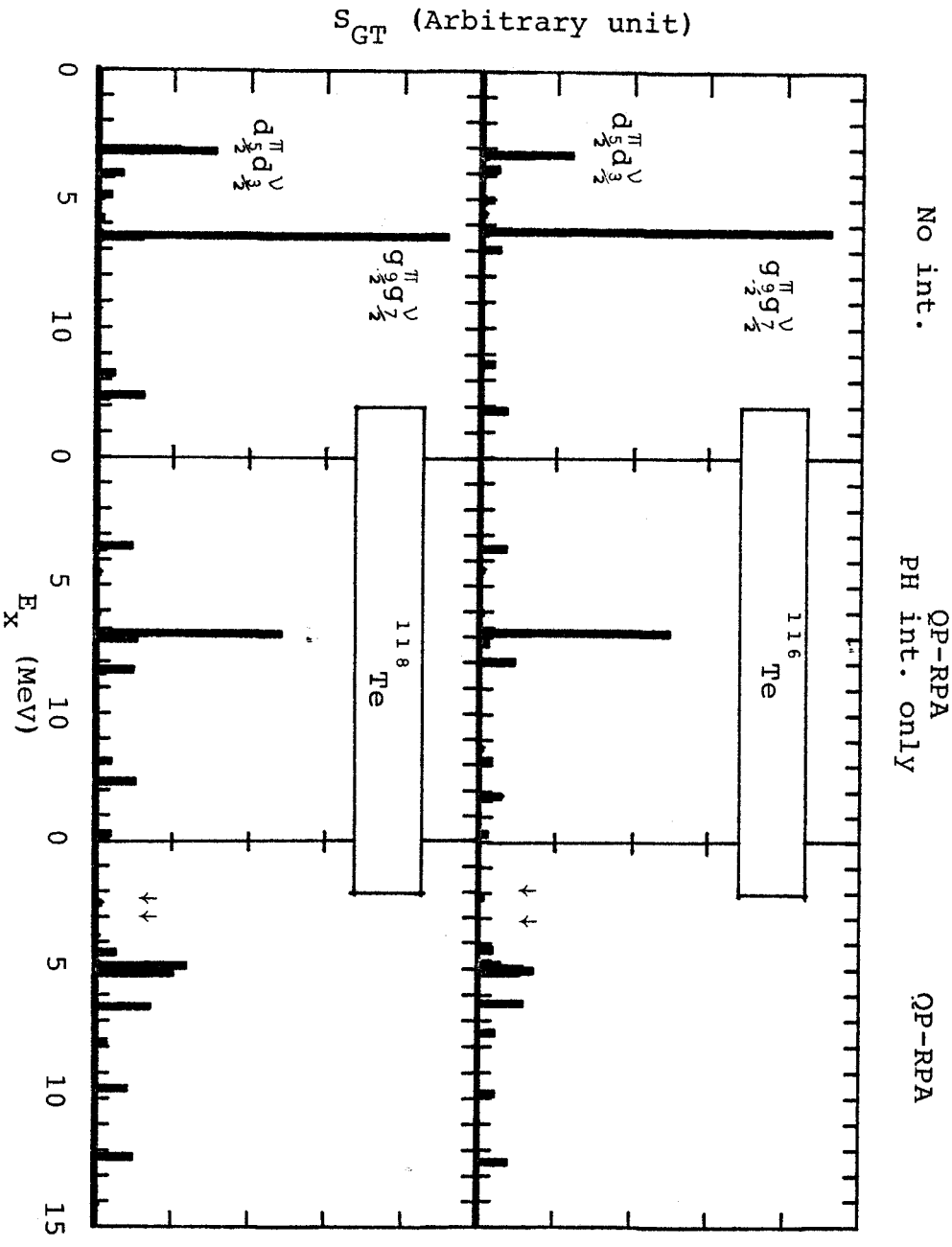

Figure 5 - Continued

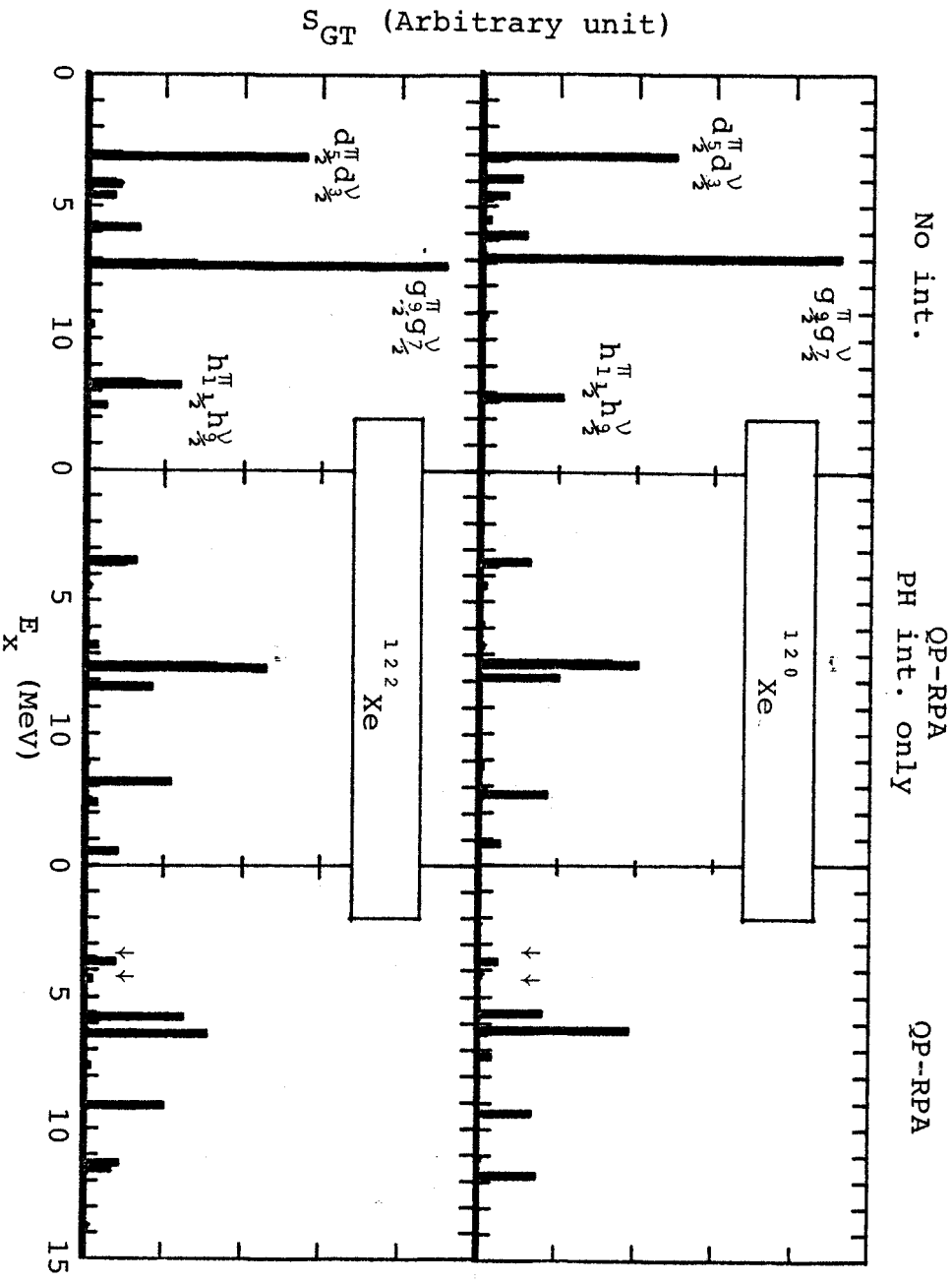

Figure 5 - Continued

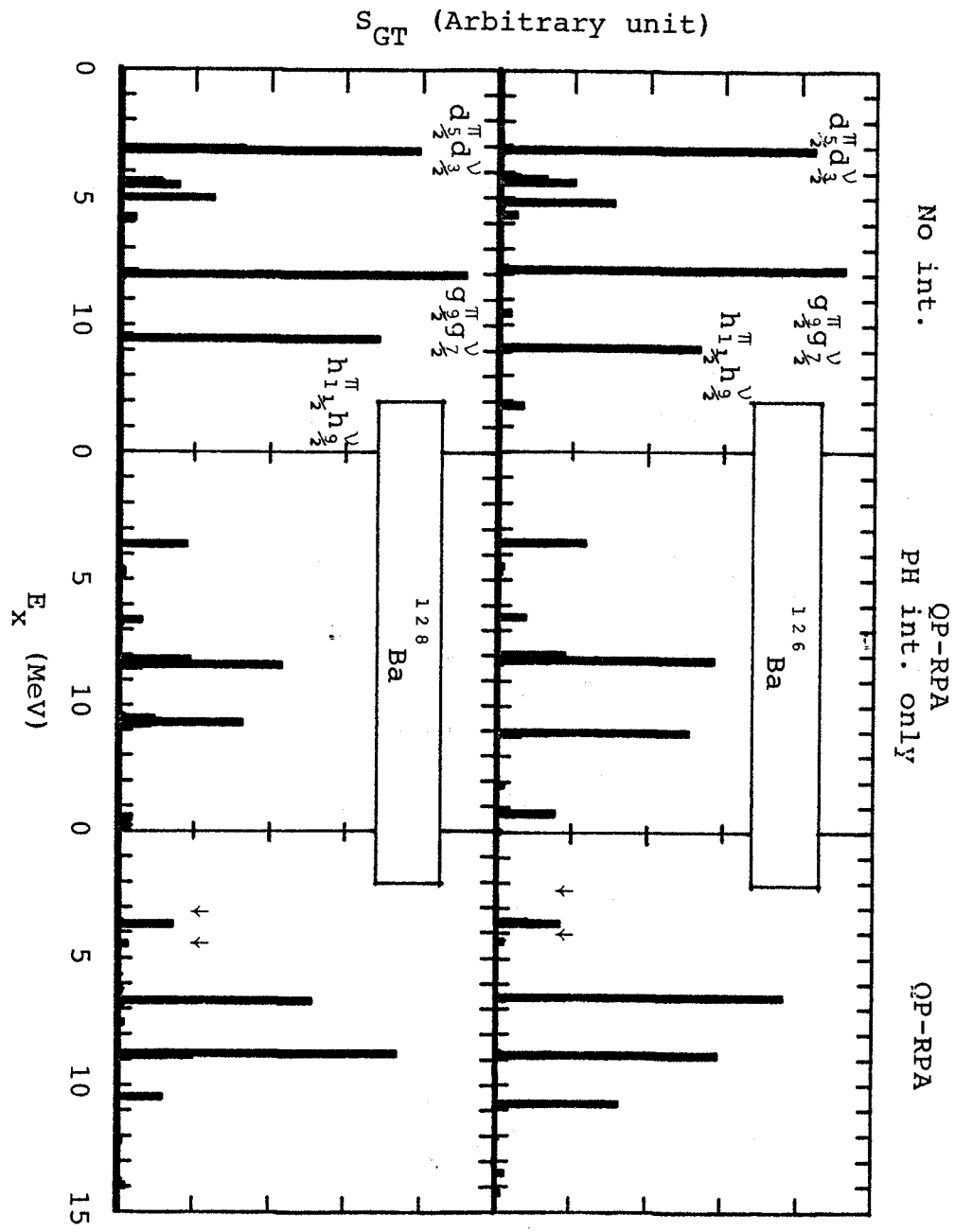

Figure 5 - Continued

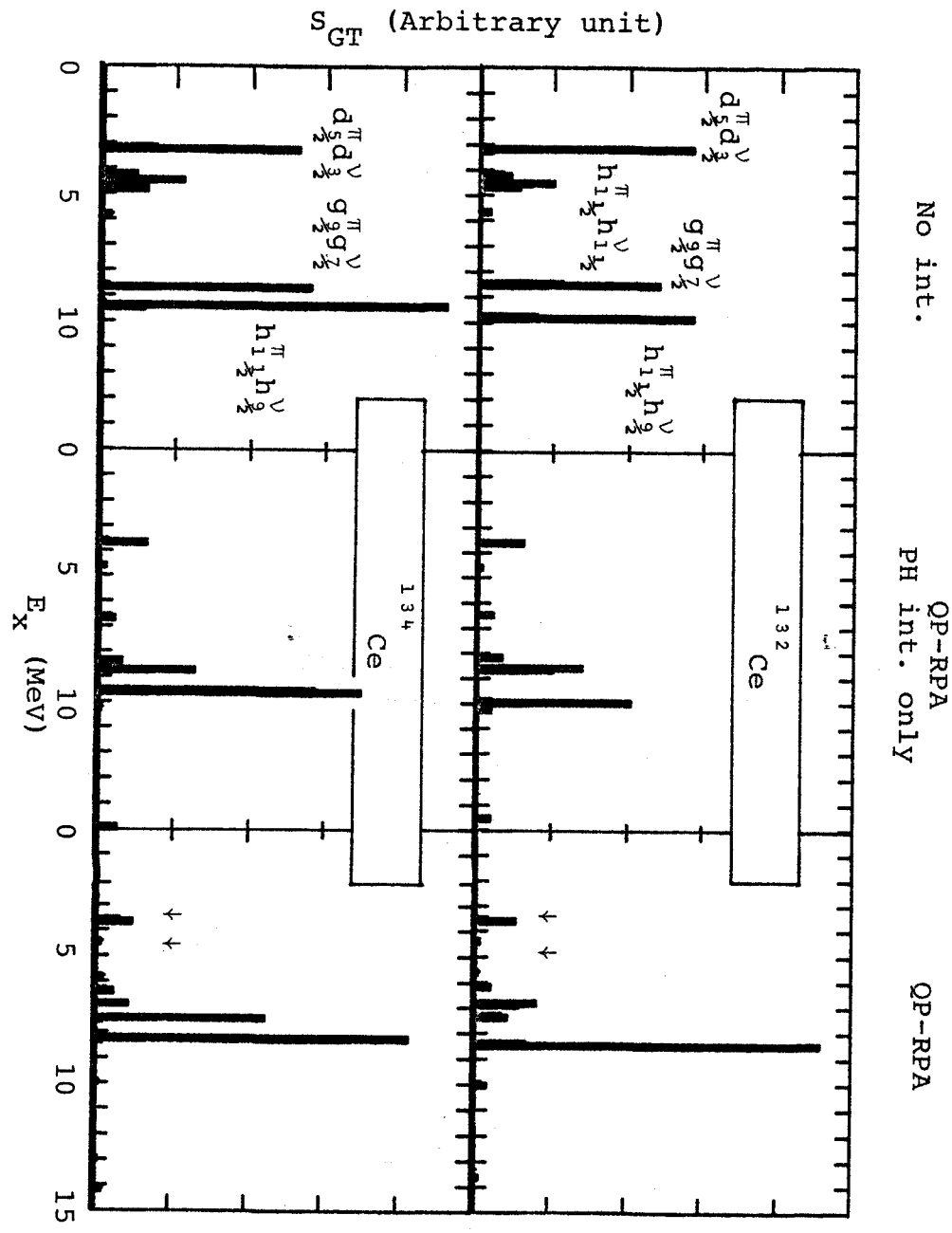

Figure 5 - Continued

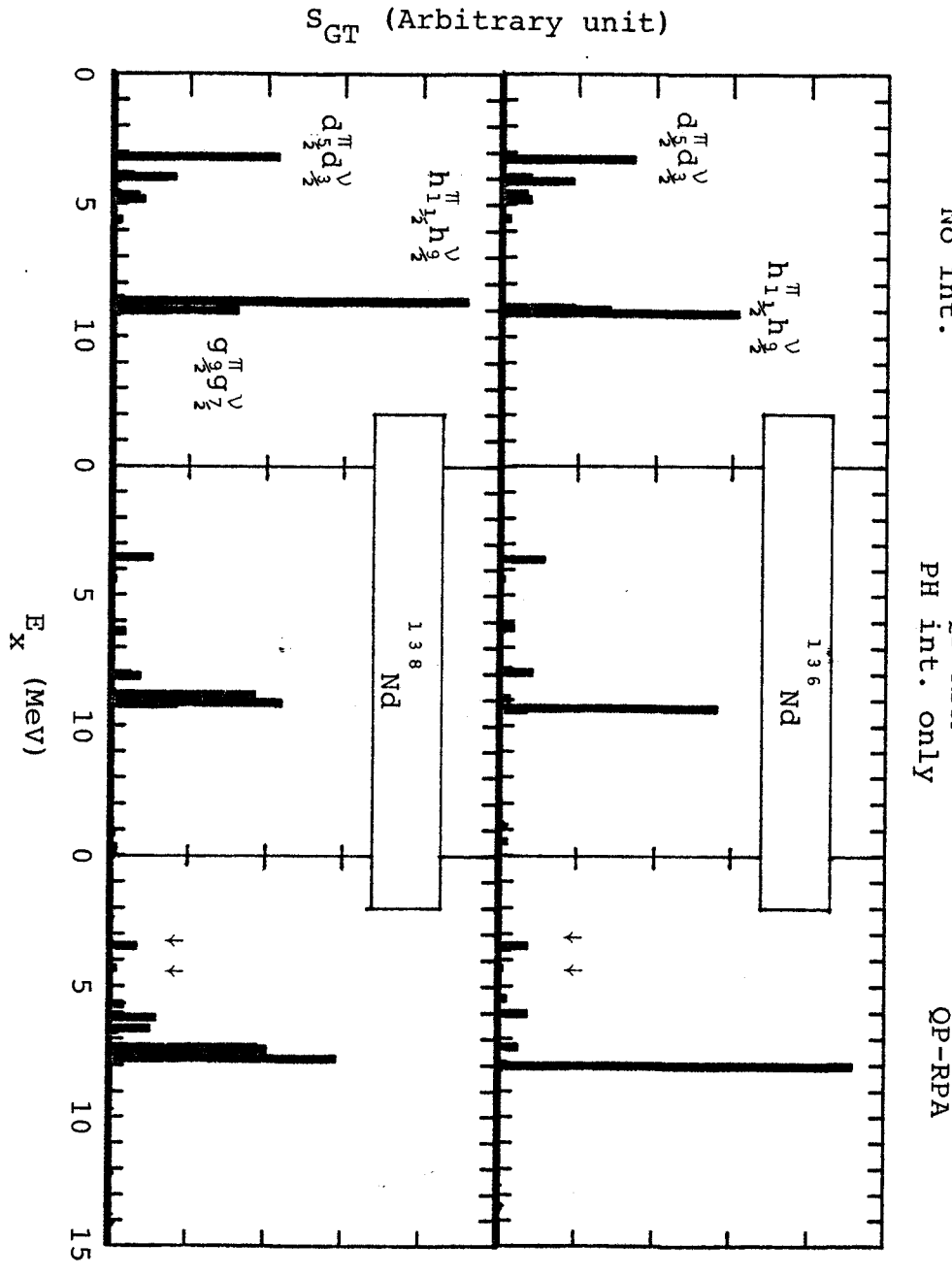

Figure 5 - Continued

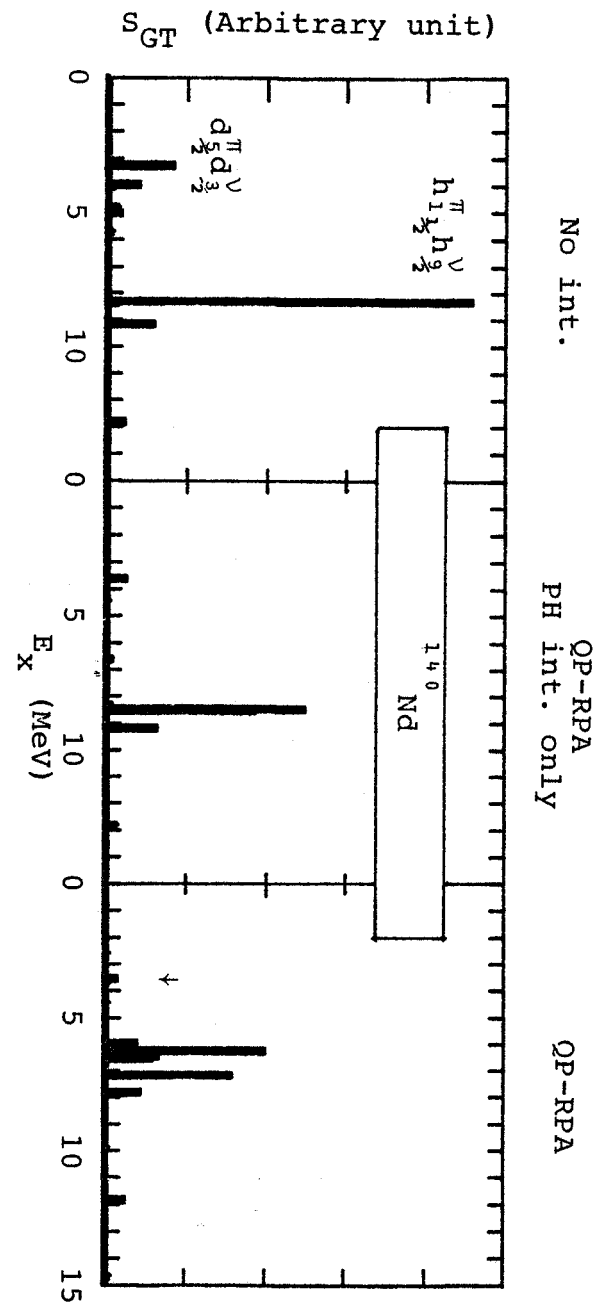

For the second half of nuclei, protons start to fill $h^{\pi}_{11/2}$ orbit and $h^{\pi}_{11/2}h^{\nu}_{9/2}$ becomes more dominant than $g^{\pi}_{9/2}g^{\nu}_{7/2}$ for cerium and neodymium isotopes. And we can find from Figure 5 that $g^{\pi}_{9/2}g^{\nu}_{7/2}$ is the lowest as well as the most dominant unperturbed state for the first group, while there are other small but not negligible unperturbed excitations lower than the most dominant state for the second group. For example, $d^{\pi}_{5/2}d^{\nu}_{3/2}$ is located lower than the $g^{\pi}_{9/2}g^{\nu}_{7/2}$ with about one-quarter of the strength of the latter in the case of ^{116}Te. This lower state appears because protons start to occupy levels above the Z=50 major shell. Also appearance of this lower state is the main reason why the second group has the transition strength one order of magnitude smaller than that of the first group.

From Figure 5, we can study the effect of interactions in more detail. With only the PH interaction, the strength function is reduced almost uniformly across the whole range of the excitation energy, while when the PP interaction is applied additionally there is not much systematic reduction of the strength. Instead, we see fragmentation of the dominant state into several weaker states or transfer of part of the strength from the lowest excitation energy to the higher excitation energy region. In the last column of Table 4, we listed the percentage of the strength which is calculated to be located above the Q-window. From that result also, we find the division due to the major

shell Z=50. The first group has about 35% of the strength above the Q-window while the second group has more than 90%. So, we predict that there would be a large concentration of the $\sigma\tau_+$ strength at higher excitation energy region that can not be observed by the β^+ decay for some of the heavy neutron rich nuclei, like the second group where the strongest unperturbed state is not the lowest state in the residual nucleus. This resonance may be found by future experiments such as a (n,p) reaction. In fact, some evidence of this sort has been already observed from the β^+ decay of odd mass nuclei. This is possible because the β decay Q-value of an odd mass nucleus is about twice as large as that of an even-even mass nucleus. For example, the β^+ decay of ^{145}Gd recently measured by Firestone et al. has shown such a structure in the strength function. [Fir82]

Finally, we want to discuss briefly about a couple of irregularities in the systematics shown in Figure 4. For most isotopes, the β^+ decay becomes less probable when the neutron number is increased. This is an obvious consequence of the Pauli blocking. However, for tin isotopes the log(ft) value of ^{110}Sn is measured to be smaller than that of ^{108}Sn. We can not find any theoretical explanation for this as yet. In xenon isotopes, the QP-RPA gives about the same strength for both of the isotopes, ^{120}Xe and ^{122}Xe, while ^{122}Xe is measured to have only one-third of the strength of ^{120}Xe. One reason for this may be the inadequacy of V_{pp} determined

by the method described in Section 4-1. If we adjusts V_{pp} to reproduce the data as close as possible, then we may have a better result. However, we did not try to adjust parameters for an individual isotope merely to have a better fit.

Chapter VI

COMPARISON WITH SHELL MODEL

6-1 Introduction

The FSM calculations have been frequently applied to the spin-flip and isospin-flip transitions. [Coh65, Bro78, Blo81, McG81] They give good agreement with the data when renormalized to account for the overall quenching of the spin dependent operators, except the 0p shell nuclei where there is no need for the renormalization. The only shortcoming of the theory seems to be its limitation on the size of nuclei which can be treated. In this chapter, we want to test the QP-RPA against the FSM calculation. One of the best candidates in this context is the 0p shell nuclei which have simple calculations and have been thoroughly studied by Cohen and Kurath. [Coh65] We take the $\sigma\tau_+$ transition of ^{12}C as the simulation for heavy neutron rich nuclei.

6-2 Simple perturbation theories vs. full-scale shell model calculation

Let us consider simple perturbation theories approached by two different schemes, the jj and LS coupling limits. To make it even simpler, we assume that every state

with even L has the same interaction energy, as does every odd L state. We will call them V_{even} and V_{odd} respectively. Then the problem is parametrized by V_{even} and V_{odd} together with single particle energies $e_{p_{1/2}}$ and $e_{p_{3/2}}$ of the $0p_{1/2}$ and $0p_{3/2}$ shells respectively.

The jj coupling scheme, which takes the residual interaction as a perturbation, is equivalent to the PH-RPA when we express the 0^+ initial state and the 1^+ final state as

$$\Psi_{jj}(0^+)=|0^+>+\alpha_{jj}|(p^{\pi}_{1/2}p^{\nu-1}_{3/2})^1(p^{\nu}_{1/2}p^{\pi-1}_{3/2})^1;0^+> \tag{6-1a}$$

$$\Psi_{jj}(1^+)=|(p^{\nu}_{1/2}p^{\pi-1}_{3/2})1^+>, \tag{6-1b}$$

where the coefficient α_{jj} is given by

$$\alpha_{jj}=-2(V_{even}-V_{odd})/(e_{p_{1/2}}-e_{p_{3/2}}). \tag{6-1c}$$

In the LS coupling scheme, where the spin-orbit force is the perturbation, we express the initial and the final states as

$$\Psi_{LS}(0^+)=|(p^4)^0(\tfrac{1}{2}^4)^0;0^+>+\alpha_{LS}|(p^4)^1(\tfrac{1}{2}^4)^1;0^+> \tag{6-2a}$$

$$\Psi_{LS}(1^+)=|(p^4)^1(\tfrac{1}{2}^4)^1;1^+>, \tag{6-2b}$$

where α_{LS} is given by

$$\alpha_{LS}=-\frac{1}{3}(e_{p_{1/2}}-e_{p_{3/2}})/(V_{even}-V_{odd}). \tag{6-2c}$$

Then the transition strength is found to be a function of an

angle defined by

$$\zeta=\tan^{-1}\left\{(V_{even}-V_{odd})/(e_{p_{1/2}}-e_{p_{3/2}})\right\}, \tag{6-3}$$

and can be expressed in two schemes by

$$B(GT;jj)=\frac{32}{9}\frac{1}{\sqrt{1+\frac{8}{9}\tan\zeta}} \tag{6-4a}$$

$$B(GT;LS)=\frac{2}{3}\frac{1}{\tan^2\zeta}\ . \tag{6-4b}$$

As for the FSM calculation, it has seventeen parameters in the complete basis of the 0p major shell, fifteen matrix elements for the two-body interaction and two single particle energies. [Coh65] We transform the two-body interaction matrix elements between the jj coupled states to those between the LS coupled ones to study in terms of the angle ζ defined by Equation (6-3). This is easily done by making use of the Racah algebra. The results are tabulated in Table 5. The columns under headings V_{even} and V_{odd} are to be understood as coefficients of the corresponding interaction energies. Then, we diagonalize the Hamiltonian by keeping V_{even} and V_{odd} fixed while adjusting the single particle energies to achieve the desired angle ζ.

The results of the three models are shown in Figure 6. The unperturbed strength for the transition from the $0p_{3/2}$ to $0p_{1/2}$ level is 32/9 as shown at $\zeta=0°$. Observe that the FSM agrees with the jj coupling scheme (PH-RPA) for

Table 5 Two-body interaction matrix elements for full-scale shell model calculation

j_1	j_2	j_3	j_4	J	T	V_{even}	V_{odd}
3/2	3/2	3/2	3/2	0	1	2/3	1/3
				1	0	4/9	5/9
				2	1	1/3	2/3
				3	0	1	0
3/2	3/2	3/2	1/2	1	0	$-\sqrt{10}/9$	$\sqrt{10}/9$
				2	1	$\sqrt{2}/3$	$-\sqrt{2}/3$
3/2	3/2	1/2	1/2	0	1	$\sqrt{2}/3$	$-\sqrt{2}/3$
				1	0	$-\sqrt{10}/9$	$\sqrt{10}/9$
3/2	1/2	3/2	1/2	1	0	7/9	2/9
				1	1	0	1
				2	0	1	0
				2	1	2/3	1/3
3/2	1/2	1/2	1/2	1	0	-2/9	2/9
1/2	1/2	1/2	1/2	0	1	1/3	2/3
				1	0	7/9	2/9

small ζ and with the LS coupling scheme for large ζ. Although we start with the expectation that the jj coupling is a good approximation in the weak interaction limit ($\zeta \to 0°$) only, it is supprising to find that it departs from the FSM very rapidly and gives a large overestimation as ζ increases. Moreover, the largest discrepancy between them appears around $\zeta \cong 50°$, which might represent the angle of the real interaction corresponding to B(GT)=0.66 which was measured by Brady et al. [Bra82] In the strong interaction

Figure 6 $\sigma\tau_+$ transition rate of three models

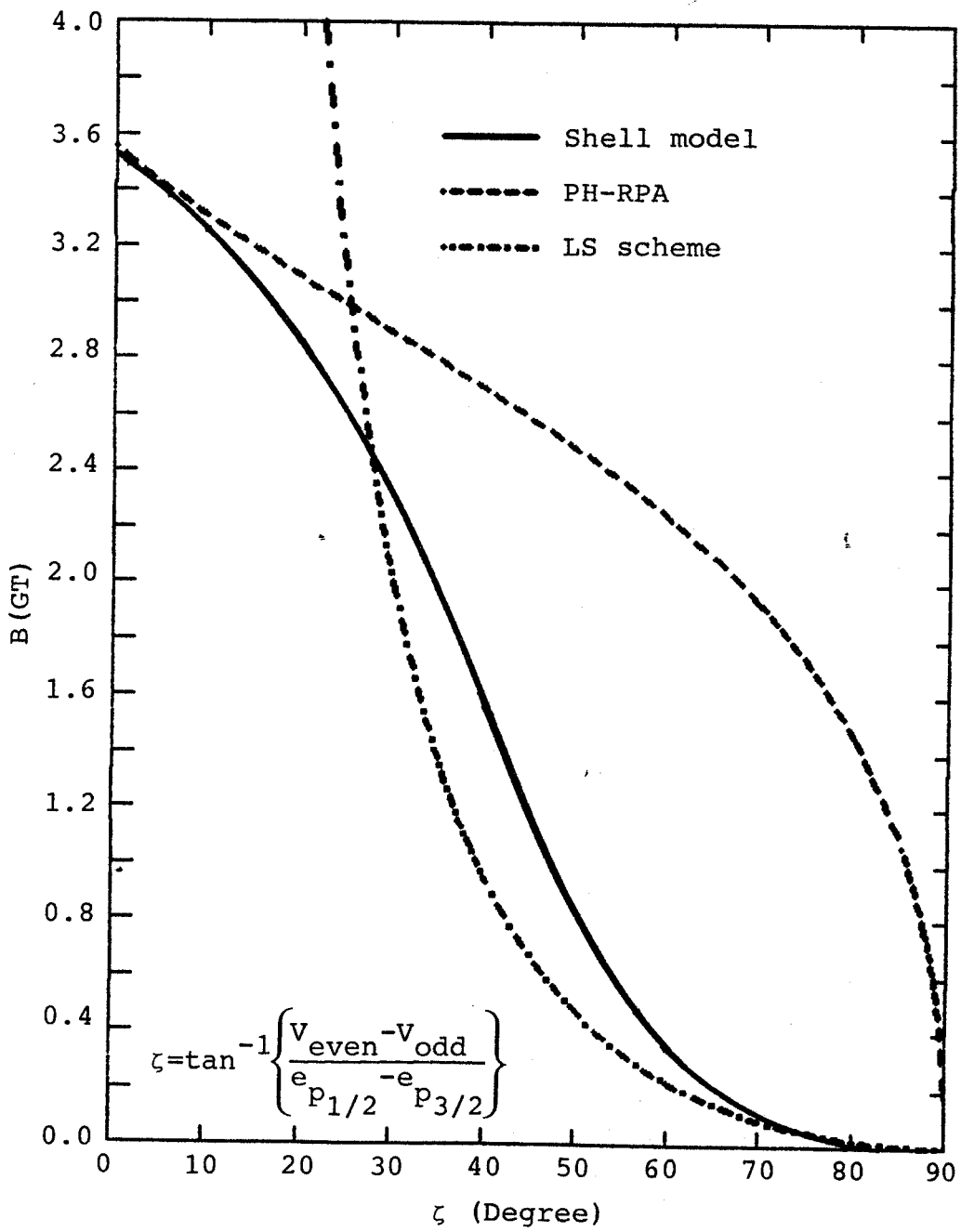

limit ($\zeta \to 90°$), all the curves approach the zero strength which reflects that there is no more distinction in energy between the $0p_{1/2}$ and $0p_{3/2}$ orbitals. But note that in the jj coupling scheme, the slope of the curve is vertical, while in the LS scheme and the FSM, the slopes are both horizontal at $\zeta = 90°$.

6-3 Quasi-particle random phase approximation vs. full scale shell model

Now, let us consider the QP-RPA. As for the single particle wavefunctions, the pairing strength of

$$G = 59.4/A \text{ MeV} \qquad (6\text{-}5)$$

is chosen to reproduce the occupation probability of the $0p_{3/2}$ and $0p_{1/2}$ orbits whose wavefunction is calculated by the Cohen-Kurath interaction. [Coh65] The PP and PH interactions are again expressed in terms of V_{even} and V_{odd}. We also redo the FSM calculation in the neutron-proton formalism rather than in the isospin formalism where the isospin is a good quantum number as was done in the last section. The neutron-proton formalism in the 0p major shell requires a total of 38 parameters. Two-body interaction matrix elements are composed of 14 elements between like nucleons and 20 elements between unlike ones, and there are four single particle energies, two for neutrons and two for protons.

Table 6 $\sigma\tau_+$ transition rates with pairing interaction only

Two-QP states	BCS	Neutron-proton shell model
$p^{\pi}_{3/2}p^{\nu}_{1/2}$	1.79	1.72
$p^{\pi}_{3/2}p^{\nu}_{3/2}$	0.68	0.70
$p^{\pi}_{1/2}p^{\nu}_{3/2}$	0.26	0.28
$p^{\pi}_{1/2}p^{\nu}_{1/2}$	0.10	0.10
	2.83	2.80

In Table 6, the QP-RPA and the neutron-proton shell model calculations are compared when there is no residual interaction between QP's. In the latter calculation, all the interaction matrix elements except those between like nculeons coupled to J=0 are set at zero, and the pairing interaction for J=0 is taken by Equation (3-1). The four two-QP states in the first column of the table are all the states one can construct from the BCS theory. We also list the lowest four states from the neutron-proton shell model calculation. They are states with seniority two. Higher states, which are mostly states with seniority greater than two, are seen to carry a negligible amount of strength. As can be seen in this table the QP-RPA reproduces the neutron-proton shell model almost exactly, when there is no residual interaction.

Because of the pairing interaction, it is not easy to define an angle like one given by Equation (6-3) consistently. Instead, we keep the pairing and single particle energies the same in both models, and assume V_{odd} is small compared to V_{even}, so we can find the transition strength in terms of V_{even} only. We plot the results in Figure 7. The solid line is the lowest state (ground state of the daughter nucleus, ^{12}B) and excitation energies are measured from this state. We show the lowest four states. We find in this figure, that the QP-RPA reproduces the neutron-proton shell model quite reasonably for both the energy and the strength except a little overestimation of the strength when V_{even} becomes large.

Finally, we calculate the QP-RPA with a short-range interaction, and compare it with the FSM calculation made with the Cohen-Kurath interaction. We use

$$V_{pp}=761 \text{ MeV fm}^3 \qquad (6\text{-}6)$$

for the strength of the PP interaction, which is determined by the method described in Section 4-1. The transition rates to the lowest four states in ^{12}B are tabulated in Table 7, together with the data by Brady et al. [Bra82] Both the theories and the data agree with the main feature that almost all the strength is concentrated in the transition to the lowest state. The Cohen-Kurath interaction reproduces the data excellently but the QP-RPA overestimates the data

Figure 7 $\sigma\tau_+$ transition rate, neutron-proton shell model vs. quasi-particle random phase approximation

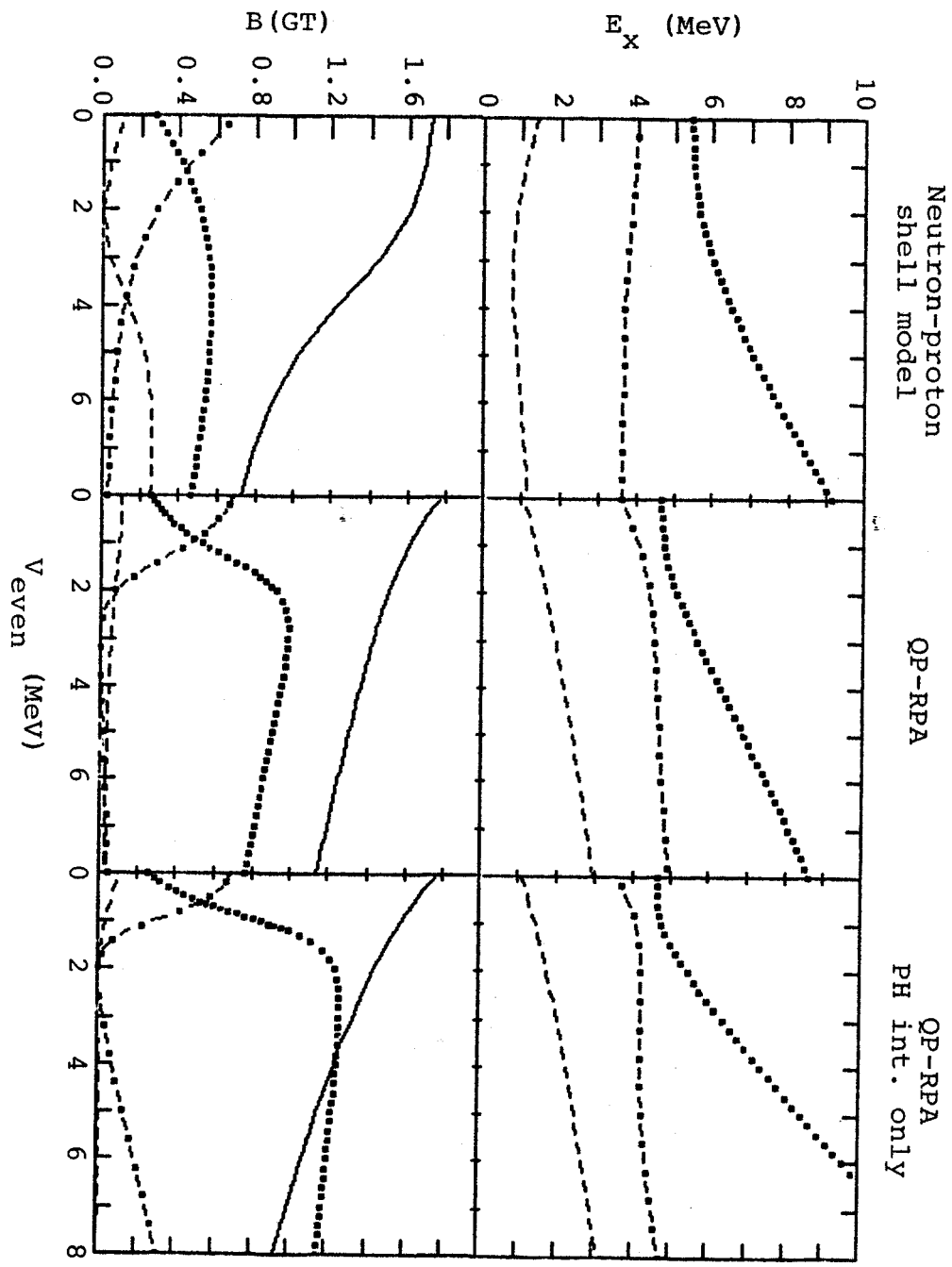

by a factor of 2.2.

6-4 Summary

As a preliminary investigation, we have tested the PH-RPA, which is derived by the simple perturbation theory, against the FSM calculation. We have found that it is good only at the small vicinity of $\zeta=0°$, which is the extreme limit of the weak interaction, and departs too much from the FSM for the angles which might correspond to the real interaction.

We then have tested the QP-RPA against the neutron-proton FSM. When the same kind of the interaction is used for both models, the QP-RPA gives a good reproduction of the FSM calculation. But when a δ-function interaction is taken

Table 7 $\sigma\tau_+$ transition rate of $^{12}C(0^+)\rightarrow{}^{12}B(1^+)$

QP-RPA		Cohen-Kurath		Experiment	
E_x	B(GT)	E_x	B(GT)	E_x	B(GT)
0.00	1.480	0.00	0.614	0.00	0.66
3.89	0.022	4.43	0.006		
4.57	0.040	6.48	0.006		
8.60	0.102	10.41	0.010		
	1.644		0.636		0.66

for the QP-RPA, it overestimates the FSM made with the Cohen-Kurath interaction, which agrees very well with the data, by 2.6 times. However, it can show the main feature that almost all the strength is concentrated in the transition to the lowest state.

Chapter VII

CONCLUSION

Motivated by the recent active research on the spin-flip and isospin-flip transitions, we have studied the $\sigma\tau_+$ transition. It is differentiated from the $\sigma\tau_-$ transition when the nucleus becomes heavy with a large neutron excess. Due to the Pauli blocking, the $\sigma\tau_+$ transition has much fewer PH configurations than $\sigma\tau_-$ while the ground state correlation is much more important in the $\sigma\tau_+$ transition than in $\sigma\tau_-$ transition.

Calculations have been performed by the QP-RPA with a simple short-range interaction. It is found that the PP interaction is quite dependent on the size of the two-QP model space used. We have adopted a simple model to determine the strength of the PP interaction for each nucleus, but a more sophisticated theory is called for. By using the PH interaction, whose strength is determined by reproducing the energy of the giant GT states, together with the PP interaction, we have found that the extra quenching of the β^+ decay rate of neutron rich even-even nuclei between mass numbers A=100$\sim$150 ranges from 1.3 to 16.3 with a reciprocal average 4.0 to reproduce the observed log(ft) values. It has been shown that the sum of the unperturbed $\sigma\tau_+$ strength is

reduced to almost half when only the PH interaction is applied. The PP interaction is shown to redistribute the strength, for example, by fragmenting the strong states which appear when only the PH interaction is applied. Therefore, the PP interaction is important in reproducing the measured log(ft) values. It has also been found that the difference in the proton configuration in the ground state of the parent nucleus causes the nuclei, which have been treated in this study, to be divided into two groups. The first group, which has protons occupying levels up to the Z=50 major shell, has the β^+ decay strength one order of magnitude larger than the second group which has protons above the major shell also. It has been predicted that for the second group, most of the strength is located above the Q-window. This is similar to the GT β^- decay whose decay rate is much hindered by the existance of the giant GT resonance at higher excitation energy.

To make sure that the QP-RPA is an adequate approximation when it is applied to the charge-exchange reaction, despite its inability to conserve the nucleon number, we have tested it against the FSM calculation for the $\sigma\tau_+$ transition of ^{12}C. When we adopt the same kind of residual interactions for both models, it reproduces the FSM reasonably well. But the QP-RPA made with the short-range interaction predicts the β^+ decay rate larger by a factor of about 2.2 than what have been measured, while the FSM with

the Cohen-Kurath interaction agrees very well with the experiment. However, the QP-RPA is able to reproduce the main feature of the $\sigma\tau_+$ strength distribution of ^{12}C, which shows that almost all the strength is concentrated in the transition to the lowest state.

In conclusion, we confirm that the strong quenching found in other spin-flip and isospin-flip transitions, is also present in the $\sigma\tau_+$ transition. The quenching factor calculated by the QP-RPA is about four on the average. But also we saw that the QP-RPA overestimates the FSM by a factor of about two for the case of ^{12}C. Therefore, it will be very interesting to measure the resonances, which are predicted by the QP-RPA, at the high excitation energy above the Q-window by future experiments like an (n,p) reaction. It will be an important check for the QP-RPA and for the amount of the quenching of the $\sigma\tau_+$ strength as well as a source of valuable information for the determination of the PP interaction.

APPENDICES

Appendix A

A SCHEME TO SOLVE

THE BARDEEN-COOPER-SCHRIEFFER EQUATIONS

We start with the single particle wavefunctions $\psi_{j\ell m}(r)$, their energies e_j, and occupation probabilities v_j^2 which are given by the usual shell model calculations such as the HF or WS single particle potential. The occupation probability v_j^2 is equal to 1 for the occupied orbits, 0 for the empty orbits, and

$$v_j^2=n/(2j+1) \tag{A-1}$$

for the Fermi orbit where it is occupied by $n<(2j+1)$ nucleons. Then we proceed as the following to obtain the BCS ground state:

i) Determine a new single particle energy e_j',

$$e_j'=e_j-Gv_j^2 \tag{A-2}$$

which comes from the pairing interaction given by Equation (3-1). [Fet71, p530]

ii) Determine the energy gap Δ and the chemical potential μ by solving the following two equation simultaneously by Newton's method, for example. [Bur78, p39]

$$\frac{4}{G}= \sum_k (2j_k+1)/\sqrt{(e'_{j_k}-\mu)^2+\Delta^2} \qquad \text{(A-3a)}$$

$$2N= \sum_k (2j_k+1)\left\{1-[e'_{j_k}-\mu]/\sqrt{(e'_{j_k}-\mu)^2+\Delta^2}\right\}. \qquad \text{(A-3b)}$$

Here, N is the number of nucleons in the model space taken for the BCS approximation.

iii) Determine a new occupation probability v_j^2,

$$v_j^2= \frac{1}{2}\left\{1-[e'_j-\mu]/\sqrt{(e'_j-\mu)^2+\Delta^2}\right\}. \qquad \text{(A-4)}$$

iv) Repeat steps i)∿iii) until one gets stationary values for Δ and μ.

Then the QP energy E_j can be obtained by

$$E_j= \sqrt{(e'_j-\mu)^2+\Delta^2}\ . \qquad \text{(A-5)}$$

Appendix B

MATRIX ELEMENTS OF THE δ-FUNCTION INTERACTION

The matrix elements of the δ-function interaction can be easily obtained by evaluating them at $\theta=0°$. [Law80, p436] The calculation is rather straightforward and we present only the final results. For the spin-independent interactions, we have

$$\begin{aligned}
&\langle [j_1(1)j_2(2)]J|\delta(r_1-r_2)|[j_3(1)j_4(2)]J\rangle \\
&= \frac{\langle R^4\rangle}{2\pi} C(j,J)\Big\{\langle j_1\tfrac{1}{2}j_2-\tfrac{1}{2}|J0\rangle(-1)^{j_1-\frac{1}{2}+\ell_1}\langle j_3\tfrac{1}{2}j_4-\tfrac{1}{2}|J0\rangle(-1)^{j_3-\frac{1}{2}+\ell_3} \\
&\quad +\langle j_1\tfrac{1}{2}j_2\tfrac{1}{2}|J1\rangle(-1)^{j_1+j_2+J}\langle j_3\tfrac{1}{2}j_4\tfrac{1}{2}|J1\rangle(-1)^{j_3+j_4+J}\Big\} \qquad \text{(B-1)}
\end{aligned}$$

$$\begin{aligned}
&\langle [j_1(1)j_2(1)^{-1}]J|\delta(r_1-r_2)|[j_3(2)j_4(2)^{-1}]J\rangle \\
&= \frac{\langle R^4\rangle}{\pi} C(j,J)\langle j_1\tfrac{1}{2}j_2-\tfrac{1}{2}|J0\rangle(-1)^{j_1-\frac{1}{2}+J}\langle j_3\tfrac{1}{2}j_4-\tfrac{1}{2}|J0\rangle \\
&\quad \times(-1)^{j_3-\frac{1}{2}+J}\delta_{J,L} \qquad \text{(B-2)}
\end{aligned}$$

$$\begin{aligned}
&\langle [j_1(1)j_2(2)^{-1}]J|\delta(r_1-r_2)|[j_3(1)j_4(2)^{-1}]J\rangle \\
&= \frac{\langle R^4\rangle}{2\pi} C(j,J)\Big\{\langle j_1\tfrac{1}{2}j_2-\tfrac{1}{2}|J0\rangle(-1)^{j_1-\frac{1}{2}+J}\langle j_3\tfrac{1}{2}j_4-\tfrac{1}{2}|J0\rangle(-1)^{j_3-\frac{1}{2}+J} \\
&\quad +\langle j_1\tfrac{1}{2}j_2\tfrac{1}{2}|J1\rangle(-1)^{j_1+j_2+\ell_1}\langle j_3\tfrac{1}{2}j_4\tfrac{1}{2}|J1\rangle(-1)^{j_3+j_4+\ell_3}\Big\}, \qquad \text{(B-3)}
\end{aligned}$$

where $\langle R^4 \rangle$ and $C(j,J)$ denote

$$\langle R^4 \rangle = \int \psi_{j_1}(r)\psi_{j_2}(r)\psi_{j_3}(r)\psi_{j_4}(r)r^2 dr \qquad \text{(B-4)}$$

$$C(j,J) = \sqrt{(j_1+\tfrac{1}{2})(j_2+\tfrac{1}{2})(j_3+\tfrac{1}{2})(j_4+\tfrac{1}{2})}/(2J+1)\,. \qquad \text{(B-5)}$$

For the spin-dependent interaction, the matrix elements become,

$$\langle [j_1(1)j_2(2)]J | \delta(r_1-r_2)\ \sigma_1\cdot\sigma_2 | [j_3(1)j_4(2)]J \rangle$$

$$= \frac{\langle R^4 \rangle}{2\pi} C(j,J) \Big\{ \langle j_1 \tfrac{1}{2} j_2 -\tfrac{1}{2} | J0 \rangle (-1)^{j_1+\ell_1-\frac{1}{2}} \langle j_3 \tfrac{1}{2} j_4 -\tfrac{1}{2} | J0 \rangle (-1)^{j_3+\ell_3-\frac{1}{2}}$$

$$\times [-3\delta_{J,L} + \delta_{J,L\pm1}] + \langle j_1 \tfrac{1}{2} j_2 \tfrac{1}{2} | J1 \rangle (-1)^{j_1+j_2+J}$$

$$\times \langle j_3 \tfrac{1}{2} j_4 \tfrac{1}{2} | J1 \rangle (-1)^{j_3+j_4+J} \Big\} \qquad \text{(B-6)}$$

$$\langle [j_1(1)j_2(1)^{-1}]J | \delta(r_1-r_2)\ \sigma_1\cdot\sigma_2 | [j_3(2)j_4(2)^{-1}]J \rangle$$

$$= \frac{\langle R^4 \rangle}{\pi} C(j,J) \Big\{ \langle j_1 \tfrac{1}{2} j_2 -\tfrac{1}{2} | J0 \rangle (-1)^{j_1-\frac{1}{2}+J} \langle j_3 \tfrac{1}{2} j_4 -\tfrac{1}{2} | J0 \rangle (-1)^{j_3-\frac{1}{2}+J}$$

$$\times \delta_{J,L\pm1} + \langle j_1 \tfrac{1}{2} j_2 \tfrac{1}{2} | J1 \rangle (-1)^{j_1+j_2+\ell_1}$$

$$\times \langle j_3 \tfrac{1}{2} j_4 \tfrac{1}{2} | J1 \rangle (-1)^{j_3+j_4+\ell_3} \Big\} \qquad \text{(B-7)}$$

$$\langle [j_1(1)j_2(2)^{-1}]J | \delta(r_1-r_2)\ \sigma_1\cdot\sigma_2 | [j_3(1)j_4(2)^{-1}]J \rangle$$

$$= -\frac{\langle R^4 \rangle}{2\pi} C(j,J) \Big\{ \langle j_1 \tfrac{1}{2} j_2 -\tfrac{1}{2} | J0 \rangle (-1)^{j_1-\frac{1}{2}+J} \langle j_3 \tfrac{1}{2} j_4 -\tfrac{1}{2} | J0 \rangle$$

$$\times (-1)^{j_3-\frac{1}{2}+J} [-3\delta_{J,L} + \delta_{J,L\pm1}] + \langle j_1 \tfrac{1}{2} j_2 \tfrac{1}{2} | J1 \rangle (-1)^{j_1+j_2+\ell_1}$$

$$\times\langle j_3\tfrac{1}{2}j_4\tfrac{1}{2}|J1\rangle(-1)^{j_3+j_4+\ell_3}\Big\} \tag{B-8}$$

where the scalar product $\sigma\cdot\sigma$ is defined by

$$\sigma\cdot\sigma=-\sigma_+\sigma_-+\sigma_o\sigma_o-\sigma_-\sigma_+. \tag{B-9}$$

The isospin part of the matrix element is not depend on space and spin coordinates, and can be factored out. The nonvanishing matrix elements of the isospin part for a neutron-proton pair state becomes,

$$\langle n(1)p(2)|\tau_1\cdot\tau_2|n(1)p(2)\rangle=-1 \tag{B-10}$$

$$\langle n(1)p(1)^{-1}|\tau_1\cdot\tau_2|n(2)p(2)^{-1}\rangle=2 \tag{B-11}$$

$$\langle n(1)p(2)^{-1}|\tau_1\cdot\tau_2|n(1)p(2)^{-1}\rangle=-1. \tag{B-12}$$

LIST OF REFERENCES

LIST OF REFERENCES

Ana81 N.Anantaraman, G.M.Crawley, A.Galonsky, C.Djalali, N.Marty, M.Morlet, A.Willis, and J-C Jourdain, Phys. Rev. Lett. 46 (1981) 1318

Ana82 N.Anantaraman, G.M.Crawley, A.Galonsky, C.Djalali, N.Marty, M.Morlet, A.Willis, J-C Jourdain, and P. Kitching, Proc. on "Nuclear physics at cyclotron and intermediate energies", (Bombay, India, 1982)

And61 J.D.Anderson and C.Wong, Phys. Rev. Lett. 7 (1961) 250

And80 B.D.Anderson, J.N.Knudson, P.C.Tandy, J.W.Watson, R. Madey, and C.C.Foster, Phys. Rev. Lett. 45 (1980) 699

Aue81 N.Auerbach, A.Klein, and N.V.Giai, Phys. Lett. 106B (1981) 347

Aue82 N.Auerbach, L.Zamick, and A.Klein, Rutger university preprint (1982)

Bai80 D.E.Bainum, J.Rapaport, C.D.Goodman, D.J.Horen, C.C. Foster, M.B.Greenfield, and C.A.Goulding, Phys. Rev. Lett. 44 (1980) 1751

Bar60 M.Baranger, Phys. Rev. 120 (1960) 957

Bec69 F.D.Becchetti Jr and G.W.Greenless, Phys. Rev. 182 (1969) 1190

Ber75 G.F.Bertsch and S.F.Tsai, Phys. Rep. 18 (1975) 125

Ber81a G.F.Bertsch, D.Cha, and H.Toki, Phys. Rev. C24 (1981) 533

Ber81b G.F.Bertsch, Nucl. Phys. A354 (1981) 157c

Ber82a G.F.Bertsch and I.Hamamoto, Phys. Rev. C26 (1982) 1323

Ber82b G.F.Bertsch, Lecture notes for Kyoto summer Inst. (Kyoto, Japan, 1982)

Blo81 S.D.Bloom, C.D.Goodman, S.M.Grimes, and R.F.Hausman Jr, Phys. Lett. 107B (1981) 336

Boh69 A.Bohr and B.R.Mottelson, "Nuclear structure" Vol.I, (Benjamin, New York, 1969)

Boh81 A.Bohr and B.R.Mottelson, Phys. Lett. 100B (1981) 10

Bra82 F.P.Brady, C.M.Castaneda, G.A.Needham, J.L.Ullmann, J.L.Romero, N.S.P.King, C.M.Morris, F.Petrovich, and R.H.Howell, Phys. Rev. Lett. 48 (1982) 860

Bro78 B.A.Brown, W.Chung, and B.H.Wildenthal, Phys. Rev. Lett. 40 (1978) 1631

Bro81 G.E.Brown and M.Rho, Nucl. Phys. A372 (1981) 397

Coh65 S.Cohen and D.Kurath, Nucl. Phys. 73 (1965) 1

Cra82 G.M.Crawley, N.Anantaraman, A.Galonsky, C.Djalali, N.Marty, M.Morlet, A.Willis, J-C Jourdain, and P. Kitching, Phys. Rev. C26 (1982) 87

Doe75 R.R.Doering, A.Galonsky, D.M.Patterson, and G.F. Bertsch, Phys. Rev. Lett. 35 (1975) 1691

Eji78 H.Ejiri and J.I.Fujita, Phys. Rep. 38 (1978) 85

Fet71 A.Fetter and J.D.Walecka, "Quantum theory of many particle systems", (McGraw Hill, New York, 1971)

Fir82 R.B.Firestone, R.C.Pardo, R.A.Warner, W.C.McHarris, and W.H.Kelly, Phys. Rev. C25 (1982) 527

Gaa80 C.Gaarde, J.S.Larsen, M.N.Harakeh, S.Y.Van der Werf, M.Igarashi, and A.Muller-Arnke, Nucl. Phys. A334 (1980) 248

Gaa82 C.Gaarde, J.Rapaport, T.N.Taddeucci, C.D.Goodman, C. C.Foster, D.E.Bainum, C.A.Goulding, M.B.Greenfield, D.J.Horen, and E.Sugarbaker, Niels Bohr Inst. preprint (1982)

Goo81 C.D.Goodman, C.C.Foster, D.E.Bainum, S.D.Bloom, C. Gaarde, J.Larsen, C.A.Goulding, D.J.Horen, T. Masterson, S.Grimes, J.Rapaport, T.N.Taddeucci, and E.Sugarbaker, Phys. Lett. 107B (1981) 406

Hal67 J.A.Halbleib Jr and R.A.Sorensen, Nucl. Phys. A98 (1967) 542

Ham65 I.Hamamoto, Nucl. Phys. 62 (1965) 49

Har81 A.Harting, W.Weise, H.Toki, and A.Richter, Phys. Lett. 104B (1981) 261

Hor80 D.J.Horen, C.D.Goodman, C.C.Foster, C.A.Goulding, M.B.Greenfield, J.Rapaport, D.E.Bainum, E.Sugarbaker, T.G.Masterson, F.Petrovich, and W.G.Love, Phys. Lett. 958B (1980) 27

Hor81 D.J.Horen, C.D.Goodman, D.E.Bainum, C.C.Foster, C. Gaarde, C.A.Goulding, M.B.Greenfield, J.Rapaport, T.N.Taddeucci, E.Sugarbaker, T.Masterson, S.M.Austin, A.Galonsky, and W.Sterrenburg, Phys. Lett. 99B (1981) 383

Ike63 K.Ikeda, S.Fujiri, and J.I.Fujita, Phys. Lett. 3 (1963) 271

Kis63 L.S.Kisslinger and R.S.Sorensen, Rev. Mod. Phys. 35 (1963) 853

Kla80 H.V.Klapdor and C.O.Wene, J.Phys. G6 (1980) 1061

Kla81 H.V.Klapdor, T.Oda, J.Metzinger, W.Hillerbrandt, and F.K.Thielemann, Z. Phys. A299 (1981) 213

Knu80 W.Knupfer, M.Dillig, and A.Richter, Phys. Lett. 95B (1980) 349

Kre81 S.Krewald, F.Osterfeld, J.Speth, and G.E.Brown, Phys. Rev. Lett. 46 (1981) 103

Lan64 A.M.Lane, "Nuclear theory", (Benjamin, New York, 964)

Lan80 A.M.Lane and J.Martorell, Ann. Phys. 129 (1980) 273

Law80 R.D.Lawson, "Theory of the nuclear shell model", (Oxford, New York, 1980)

Led78 C.M.Lederer and V.S.Shirley, "Table of isotopes", 7th edition, (John Wiley & Sons, New York, 1978)

Lov81 W.G.Love and M.A.Franey, Phys. Rev. C24 (1981) 1073

McG80 J.B.McGrory and B.H.Wildenthal, Ann. Rev. Nucl. Part. Sci. 30 (1980) 383

McG81 J.B.McGrory and B.H.Wildenthal, Phys. Lett. 103B (1981) 173

Mey81 J.Meyer-Ter-Vehn, Phys. Rep. 74 (1981) 323

Nak82 K.Nakayama, A.P.Galeao, and F.Krmpotic, Phys. Lett. 114B (1982) 217

Ori81 H.Orihara, T.Murakami, S.Nishihara, T.Nakahawa, K. Maeda, K.Miura, and H.Ohnuma, Phys. Rev. Lett. 47 (1981) 301

Ose79 E.Oset and M.Rho, Phys. Rev. Lett. 42 (1979) 47

Ost81 F.Osterfeld, T.Suzuki, and J.Speth, Phys. Lett. 99B (1981) 75

Ost82 F.Osterfeld, S.Krewald, J.Speth, and T.Suzuki, Phys. Rev. Lett. 49 (1982) 11

Row68 D.J.Row, Rev. Mod. Phys. 40 (1968) 153

Sag82 S.Sagawa and N.V.Giai, Phys. Lett. 113B (1982) 119

San76 T.S.Sandhu and L.Rustgi, Phys. Rev. C14 (1976) 675

Sha74 A.deShalit and H.Feshbach, "Theoretical nuclear physics", (John Wiley & Sons, New York, 1974)

Spe80 J.Speth, V.Klemt, J.Wambach, and G.E.Brown, Nucl. Phys. A343 (1980) 382

Ste80 W.A.Sterrenberg, S.M.Austin, R.P.Devito, and A. Galonsky, Phys. Rev. Lett. 45 (1980) 1839

Suz81 T.Suzuki, Nucl. Phys. A379 (1982) 110

Tok81 H.Toki, D.Cha, and G.F.Bertsch, Phys. Rev. C24 (1981) 1371

Tok82 H.Toki and G.F.Bertsch, To be published in Phys. Rev. C

Tsa78 S.F.Tsai, Phys. Rev. C17 (1978) 1862

Wap71 A.H.Wapstra and N.B.Gove, Nucl. Dat. Tabl. 9 (1971) 265

Wei82 W.Weise, Proc. Int. Conf. "Spin excitations in nuclei", (Telluride, Tennessee, 1982)